



# Discovery of novel BTK PROTACs for B-Cell lymphomas

Yunpeng Zhao <sup>a,1</sup>, Yongzhi Shu <sup>b,1</sup>, Jun Lin <sup>c</sup>, Zhendong Chen <sup>b</sup>, Qiong Xie <sup>a</sup>, Yanning Bao <sup>a</sup>, Lixue Lu <sup>a</sup>, Nannan Sun <sup>a,d,\*\*</sup>, Yonghui Wang <sup>a,\*</sup>

<sup>a</sup> Department of Medicinal Chemistry, School of Pharmacy, Fudan University, 826 Zhangheng Road, Shanghai, 201203, China

<sup>b</sup> Shanghai Meizer Pharmaceuticals Co., Ltd, 58 Yuanmei Road, Shanghai, 201109, China

<sup>c</sup> School of Pharmaceutical Sciences, Jiangnan University, 1800 Lihu Avenue, Wuxi, 214122, China

<sup>d</sup> Key Laboratory of Advanced Drug Preparation Technologies, Ministry of Education, School of Pharmaceutical Sciences, Zhengzhou University, Zhengzhou, 450001, China

## ARTICLE INFO

### Article history:

Received 8 July 2021

Received in revised form

31 August 2021

Accepted 31 August 2021

Available online 2 September 2021

### Keywords:

BTK

PROTACs

B-Cell Lymphomas

ARQ531

Protein degradation

## ABSTRACT

Bruton's tyrosine kinase (BTK) is a key drug target for B-cell related malignancies. Irreversible covalent BTK inhibitors have been approved for the treatment of B-cell malignancies, yet BTK C481S mutation at the covalent binding site has caused drug-resistance of BTK covalent binding inhibitors. The proteolysis targeting chimera (PROTAC) technology increases the sensitivity to drug-resistant targets compared to classic inhibitors, which provides a new strategy for mutant BTK related B-cell malignancies. ARQ531, a reversible non-covalent BTK inhibitor that inhibits wild type (WT) and mutated BTK with high selectivity, could be an ideal warhead for PROTACs targeting the mutant BTK. Herein, we designed a novel series of PROTACs using the selective non-covalent BTK inhibitor ARQ531 as warhead, with the goal of improving the degradation of both wild-type and C481S mutant BTKs, and increasing the selectivity of BTK over other kinases. This effort will provide some basis for further preclinical study of BTK PROTACs as a novel strategy for treatment of B-cell lymphomas.

© 2021 Elsevier Masson SAS. All rights reserved.

## 1. Introduction

B-cell malignancies are different kinds of lymphomas affecting B cells, such as mantle cell lymphoma (MCL), diffuse large B-cell lymphoma (DLBCL), chronic lymphocytic leukemia (CLL), and Waldenstrom's macroglobulinemia (WM) [1]. BTK is a member of tyrosine kinase expressed in hepatocellular carcinoma (TEC) family, many B-cell leukemias and lymphomas [2,3]. Besides, it is a key regulator in the B-cell receptor (BCR) signaling pathway, therefore, BTK associates with abnormal B-cell proliferation and it is regarded as an attractive target for B-cell malignancies [4]. Ibrutinib, acalabrutinib and zanubrutinib are approved drugs that inhibit BTK [5–7]. These BTK inhibitors that irreversibly and covalently bound to C481 in the ATP binding pocket of BTK have shown positive effects in CLL, MCL and several other B-cell malignancies, but the

covalently binding inhibitors such as ibrutinib could promote resistance in patients and thus associate with poor prognosis [8]. C481, T474 and T316 are the mostly found mutations in patients with ibrutinib-resistance [9,10]. The BTK C481S is the most common mutation, which accounts for more than 80% CLL patients who have attained resistance to ibrutinib [11].

The PROTAC approach functions in an event-driven pharmacology manner instead of an occupy-driven pharmacology manner, which is a novel drug discovery strategy for degrading some undruggable targets and targeting on the proteins with resistant mutations [12,13]. PROTACs work as heterobifunctional small molecules by recruiting both an E3 ubiquitin ligase and target protein. The ternary complex induces the ubiquitination on target protein and leads to subsequent degradation by the proteasome [14,15]. Utilizing the degradation mechanism, PROTACs could overcome the potential resistance caused by persistent inhibitor treatments. Developing BTK PROTACs is a promising strategy to regulate BCR signaling pathway because the degradation instead of inhibition could effectively enhance the sensitivity to ibrutinib-resistant BTK mutant.

In recent years, quite a few PROTACs targeting BTK have been reported, but most of them share ibrutinib and its analogs as the

\* Corresponding author.

\*\* Corresponding author. Department of Medicinal Chemistry, School of Pharmacy, Fudan University, 826 Zhangheng Road, Shanghai, 201203, China.

E-mail addresses: [nysnn@126.com](mailto:nysnn@126.com) (N. Sun), [yonghuiwang@fudan.edu.cn](mailto:yonghuiwang@fudan.edu.cn) (Y. Wang).

<sup>1</sup> Both authors contributed equally.

warhead [16–22]. The irreversible covalent inhibitor achieving high target occupancies largely depends on the strong covalent binding affinity, and such binding mode may lead to non-catalytic degradation of target proteins because the irreversible covalent PROTACs are consumed once they bind to their targeted protein [17]. The reversible non-covalent PROTACs with ibrutinib analog warheads were also designed. Comparing structurally similar covalent PROTACs with non-covalent PROTACs, weaker BTK degradation of non-covalent PROTACs was found [17,20]. The attenuated efficient BTK degradation of these reversible non-covalent PROTACs with ibrutinib analog warheads is assumed for their mild binding affinity due to the loss of covalent bond [17]. Recently, some structurally distinct new non-covalent BTK inhibitors have been discovered showing potent inhibitory activity against both WT and C481S BTK [23]. ARQ531 is a potent, reversible inhibitor (BTK<sup>WT</sup> IC<sub>50</sub> = 0.85 nM, BTK<sup>C481S</sup> IC<sub>50</sub> = 0.39 nM) with activities against BTK C481S-mutated CLL cells [24,25]. Both the WT and C481S BTK binding affinity of ARQ531 is high because of its unique binding mode. ARQ531 reversibly binds to BTK, not interacting with C481, which suggests that C481S mutation would not affect the binding [26]. ARQ531-based PROTACs would better keep the high binding affinity compared to the ibrutinib-based non-covalent PROTACs, in which the covalent bond contributes a lot in binding affinity. What's more, ARQ531-based PROTACs could also avoid the non-catalytic degradation of ibrutinib-based irreversible covalent PROTACs. Thus, the efficient reversible binding mode indicating that ARQ531 could be an ideal warhead for PROTACs targeting BTK, especially the mutant BTK. Herein, we describe the design and synthesis of a series of novel BTK PROTACs based the reversible non-covalent BTK inhibitor ARQ531. Additionally, protein degradation was examined via Western blot analysis to select compounds. These efforts have led to the discovery of potent and structurally distinct BTK PROTACs as leads for development of novel and potent BTK PROTACs for treatment B-cell lymphomas.

## 2. Results and discussion

### 2.1. Design and synthesis of PROTACs based on ARQ531

For the design of the ARQ531-based PROTACs, we firstly scrutinized the binding mode of ARQ531. The cocrystal structure of BTK in complex with ARQ531 shows that ARQ531 inhibits BTK and does not interfere with C481 (PDB ID: 6E4F, Fig. 1a) [25]. The tetrahydropyran methanol is exposed to the solvent area forming hydrogen bond with N484, the middle pyrrolopyrimidine moiety forms hydrogen bonds with the backbone of E475 and M477, and the phenoxyphenyl group lays in the hydrophobic pocket of the ATP binding region. Based on such binding mode, we designed several warheads mainly modifying the tetrahydropyran methanol moiety, for easily welding the linker together and keeping the BTK binding affinity. At the beginning, carboxyethyl (compound **2**) and 4-aminocyclohexyl (compound **5**) were chosen to replace the chiral tetrahydropyran methanol moiety. Then, considering the synthetic ease of connecting warhead and linker while maintaining BTK binding affinity, we added some small linkage moieties to compound **2** and compound **5** to obtain compounds **3**, **4** and **6**. The impact of the linking moieties on BTK binding affinities were also analyzed. The 4-aminocyclohexyl-containing compounds **5** and **6** were found to be better BTK inhibitors than carboxyethyl-containing compounds **2–4** (Table 1), as **5** and **6** might provide a hydrogen bond with N484 that is in spatial proximity to the hydrogen bond formed by compound **1** (ARQ531). Binding affinities of compound **4** (IC<sub>50</sub> = 407.1 nM) and compound **6** (IC<sub>50</sub> = 25.2 nM) were found to be reasonable compared to compound **2** (IC<sub>50</sub> = 81.4 nM) and compound **5** (IC<sub>50</sub> = 4.3 nM), respectively,

indicating the possibilities of maintaining the BTK binding affinities as the linkers are introduced. Thus, we chose compounds **4** and **6** as the warheads which can easily connect and extend the linkers in design of BTK PROTACs.

The previous works displayed the wide application of CRBN E3 ligase binder in PROTACs [26–29], thus, we choose pomalidomide as E3 ligase binder. Then, the compounds **4** and **6**, as warhead A and warhead B, were separately joined to pomalidomide by PEG-linkers of various lengths to form novel PROTACs targeting BTK (Fig. 1b).

The synthesis of the designed BTK PROTACs was shown in Schemes 1–3. First, in order to synthesize various PROTACs with different linkers, a library of the key intermediates **A3a–A3b**, **A4a–A4f** was prepared as in Scheme 1. The synthesis of the key intermediates **A3a–A3b**, **A4a–A4f** began with condensation reaction of **A1**. Nucleophilic substitution of **A2** with the amino of various linkers and subsequent deprotection of the -Boc group gave the key intermediates **A3a–A3b** and **A4a–A4f**.

The synthesis of warheads **2–6** was outlined in Scheme 2. **B2** was obtained through nucleophilic substitution of **B1** with phenol, followed by hydrolysis of **B2** to produce the intermediate **B3**. Esterification of **B3** with iodomethane in the presence of K<sub>2</sub>CO<sub>3</sub> gave the intermediate **B4**. **B5** was synthesized by acylation of **B4** with 5-bromo-4-chloro-7H-pyrrolo[2,3-d]pyrimidine in the presence of *n*-BuLi. A substitution reaction of **B5** with *tert*-butyl glycinate or *tert*-butyl ((1*S*,4*S*)-4-aminocyclohexyl)carbamate in the presence of DIPEA, and subsequent deprotection of the Boc group gave the warheads **2** or **5**, respectively. Warhead **3** was obtained by substitution reaction of **B5** with ethyl glycinate in the presence of DIPEA. Amidation of the warhead **2** and ethylamine generated the warhead **4**, and warhead **5** condensed with ethylamine gave the warhead **6**.

The synthesis of BTK PROTACs was shown in Scheme 3. Compounds **4a–4h** were synthesized by the amidation of intermediate **2** and the CRBN ligase ligand conjugated linkers (**A3a–A3b**, **A4a–A4f**). Warhead **5** was condensed with various CRBN ligase ligand conjugated linkers (**A3b**, **A4a–A4d**) to generate the compounds **6a–6e**.

### 2.2. PROTACs degrade BTK<sup>WT</sup> and BTK<sup>C481S</sup>

We first determined the BTK binding affinities of our PROTACs and used ARQ531 as the reference compound. The warhead-A (compound **4**) based PROTACs showed decreased BTK binding affinities, with IC<sub>50</sub> of 1209.5 nM–3775.0 nM, which are about 3–9 folds reduction compared to compound **4** (Table 2). Interestingly, the length of linker affects the BTK binding affinity of PROTAC. PROTACs **4a**, **4b** and **4c** weakly inhibit BTK probably due to the steric clash. As the linkers became longer, PROTACs **4f** and **4g** showed improved BTK inhibition. This SAR of BTK binding affinity is consistent with that in the previous report [20]. Then, we performed quantitative Western blot to measure the levels of PROTAC-mediated BTK degradation in JeKo-1 cells, which is a human mantle cell lymphoma cell line (Fig. 2). The degradation results are generally consistent with the BTK inhibition results (Table 2). Not surprisingly, ARQ531 showed no degradation activity as the warhead. PROTACs with short linker (**4a**, **4b** and **4c**) presented a poor degradation. **4d** and **4e** displayed good BTK degradation activity with the DC<sub>50</sub> of 28.5 nM and 9.4 nM respectively, but the maximal percent of degradation are as low as 67.1% and 66.5%. As the linker grows, the activity of BTK degradation keeps increasing. PROTACs **4f** and **4g** degraded BTK effectively (DC<sub>50</sub> = 8.1 and 8.3 nM) with the maximal degradation of 72.4% and 92.4%. PROTAC **4h** with a 23-atom linker weakly degraded BTK. Such results indicated that in warhead-A based PROTACs, the linker length with 20 atoms is proper for BTK degradation.

Next, we examined the BTK inhibition and degradation of

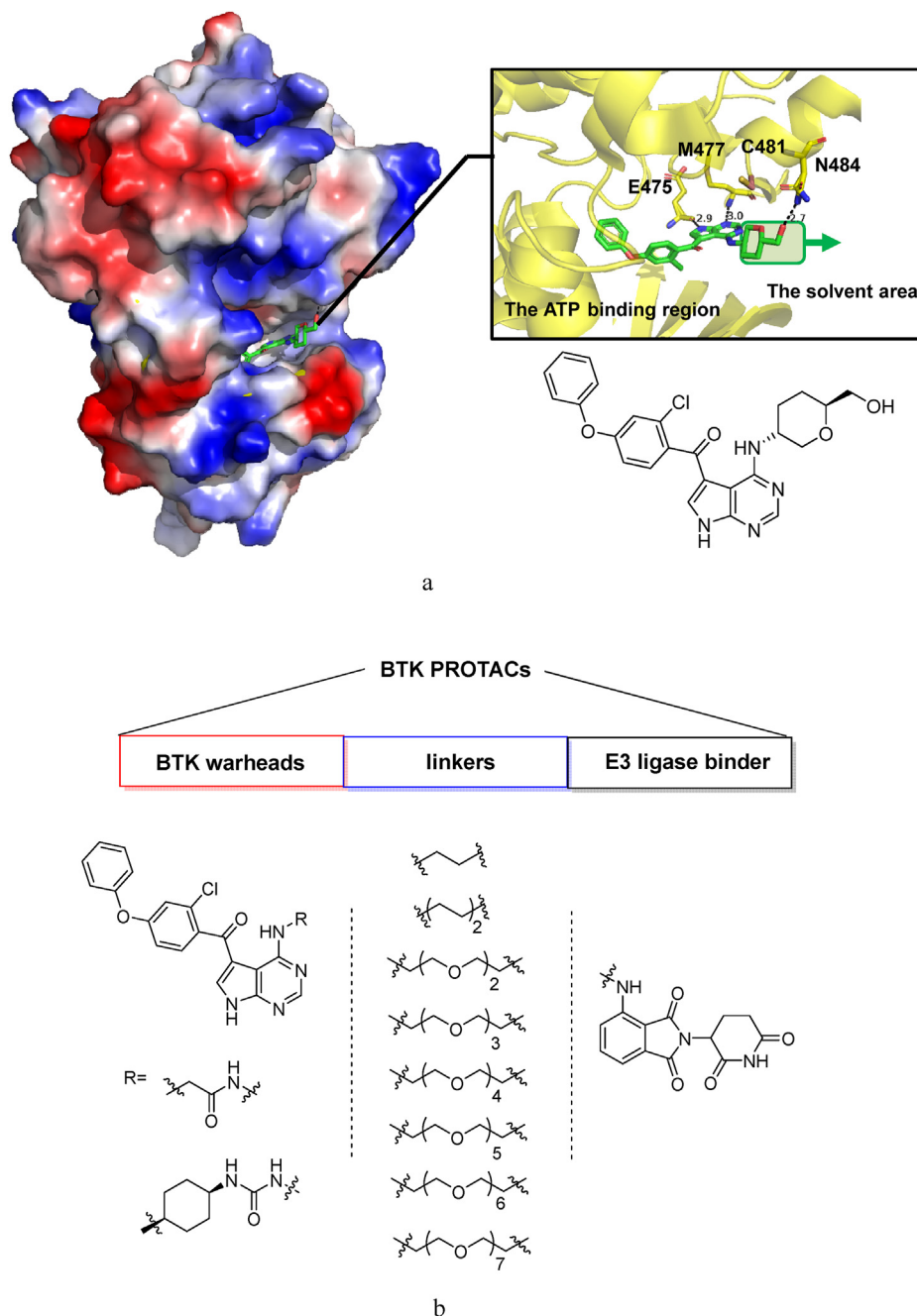


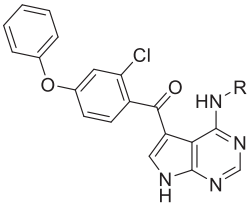
**Fig. 1.** (a) The binding mode of ARQ531 in complex with BTK (PDB ID: 6E4F [26]). (b) Design of novel BTK PROTACs.

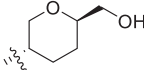
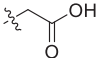
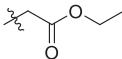
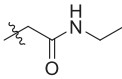
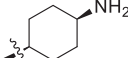
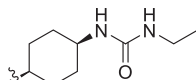
warhead-B (compound **6**) based PROTACs. The BTK binding SAR of these PROTACs is similar to warhead-A based PROTACs. The warhead-B based PROTACs showed less decreased BTK binding affinities, which are about 0.6–2.2 folds reduction compared to compound **6** (Table 3). The binding affinity of PROTAC **6c** ( $IC_{50} = 22.3$  nM) is comparable to that of compound **6** ( $IC_{50} = 25.2$  nM). This remained potency may be due to the higher binding affinity of the warhead B which could keep the stronger interaction with BTK. Then we explored the degradation of warhead-B based PROTACs. PROTACs **6a** and **6b** difficultly degrade BTK even at 1000 nM. **6c–6e** showed potent BTK degradation with concentration-dependent reduction in BTK levels with an approximate  $DC_{50}$  of 12.1 nM–41.9 nM, respectively (Fig. 3), and **6e** with long linker (17 atoms length) is the most potent PROTAC

( $D_{max} = 93.0\%$ ).

To test our hypothesis that the potent PROTACs could effectively degrade the mutated BTK in cells, we carried out the BTK degradation of selected PROTACs on a cultured BTK<sup>C481S</sup> TMD8 cell line. The results showed that the reversible non-covalent BTK warhead based PROTACs could effectively degrade the C481S mutant BTK with  $DC_{50}$  of 30.1 nM–80.4 nM in a concentration-dependent manner (Fig. 4 and Table 4). The warhead-A based PROTACs have weaker activities on BTK<sup>C481S</sup> degradation than on BTK<sup>WT</sup> degradation. Taking the most potent warhead-A based PROTAC **4g** as an example, the BTK<sup>C481S</sup>  $DC_{50}$  is 52.3 nM, which is about 6-folds less than that on WT BTK. The  $D_{max}$  on BTK<sup>C481S</sup> degradation is similar with that on BTK<sup>WT</sup> (84.8% vs 92.4%). The warhead-B based PROTACs are more potent PROTACs than warhead-A based ones. The

**Table 1**  
BTK binding affinity of the designed warheads.

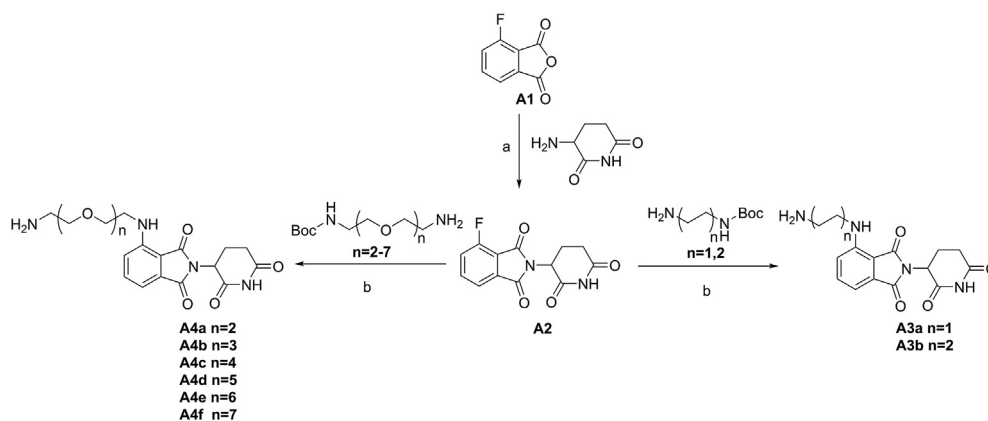


Compd.	R group	BTK inhibition (%) <sup>1,2</sup>		IC <sub>50</sub> <sup>1,2</sup> (BTK <sup>WT</sup> , nM)
		@50 nM	@500 nM	
<b>1</b> (ARQ531)		89.5 ± 0.5	98.7 ± 0.1	8.2 ± 0.7
<b>2</b>		44.2 ± 1.4	85.1 ± 0.3	81.4 ± 5.7
<b>3</b>		4.9 ± 4.7	10.9 ± 7.2	5968.0 ± 1118.6
<b>4</b>		ND <sup>3</sup>	ND <sup>3</sup>	407.1 ± 44.2
<b>5</b>		94.2 ± 0.2	99.5 ± 0.3	4.3 ± 0.5
<b>6</b>		ND <sup>3</sup>	ND <sup>3</sup>	25.2 ± 5.1

<sup>1</sup> The biochemical BTK inhibition (BTK Inhibition IC<sub>50</sub>) was measured by Shanghai ChemPartner Co., Ltd.

<sup>2</sup> BTK inhibition and IC<sub>50</sub> values are the average of at least two determinations.

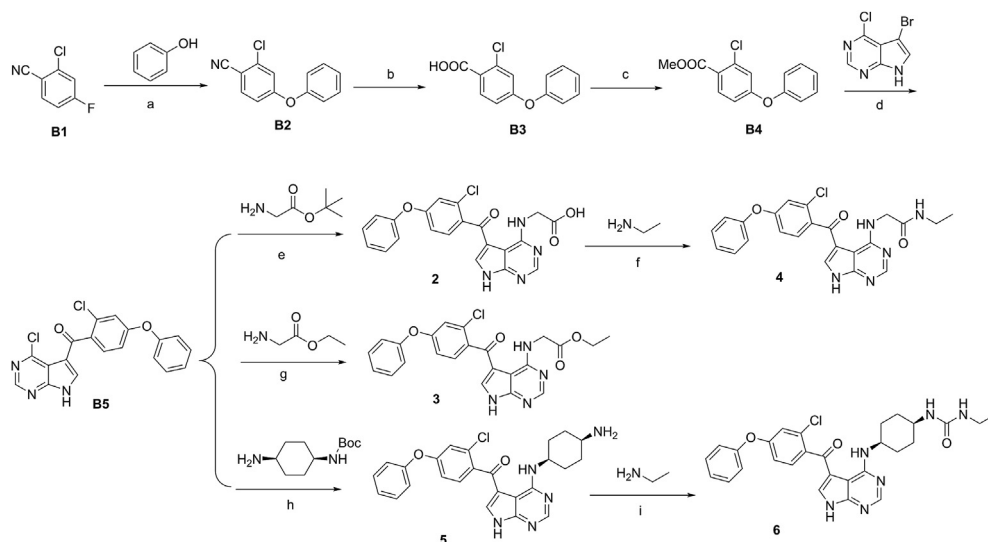
<sup>3</sup> ND: not determined.



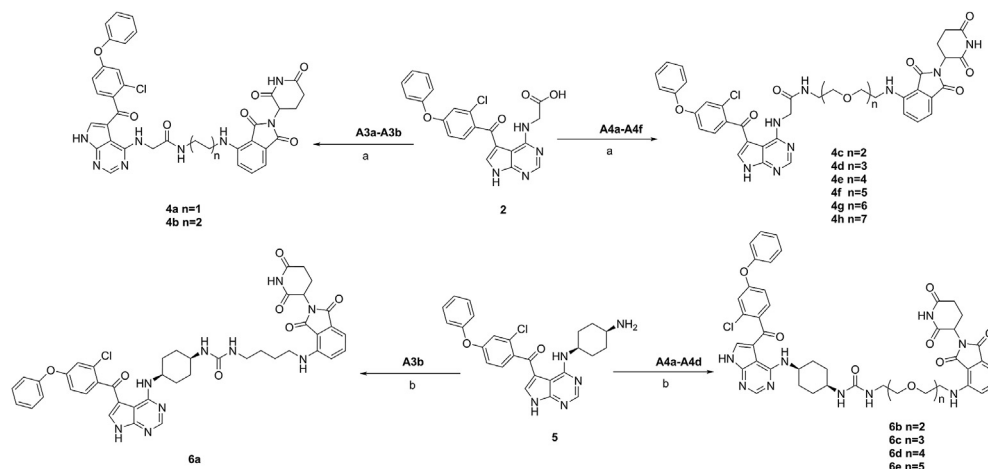
warhead-B based PROTACs **6c**, **6d** and **6e** have the BTK<sup>C481S</sup> DC<sub>50</sub> of 30.1 nM, 37.9 nM and 42.9 nM ( $D_{\max}$  is 83.5% – 90.7%), respectively, which are comparable to those of BTK<sup>WT</sup> degradation.

It is interesting that both the PROTACs with strong BTK binding activity and with weak BTK binding activity could possess potent BTK degradation, i.e., **4g** and **6e**. The higher BTK binding affinity

seems beneficial for the BTK-PROTAC-CRBN ternary complex formation. The less BTK binding affinity also executes the ternary complex formation, accounting for the event-drive mechanism of PROTACs. But so far, the exact mechanism associated with the protein inhibition and degradation was not very clear.



**Scheme 2.** Reagents and conditions: (a) NaH, DMF, rt, 1 h; (b) NaOH, EtOH/H<sub>2</sub>O, 85 °C, 16 h; (c) Iodomethane, K<sub>2</sub>CO<sub>3</sub>, DMF, rt, 1 h; (d) *n*-BuLi, THF, -78 °C, 3 h; (e) (1) DIPEA, IPA, 85 °C, 3 h; (2) TFA, DCM, rt, 1 h; (f) DIPEA, DMF, HATU, rt, 2 h; (g) DIPEA, IPA, 85 °C, 3 h; (h) (1) DIPEA, IPA, 85 °C, 3 h; (2) TFA, DCM, rt, 1 h; (i) DIPEA, THF, triphosgene, 0 °C-rt, 1 h.



**Scheme 3.** Reagents and conditions: (a) DIPEA, DMF, HATU, rt, 2 h; (b) DIPEA, THF, triphosgene, 0 °C-rt, 1 h.

### 2.3. The cell proliferation inhibition potency of BTK PROTACs in TMD8 cells and BTK<sup>C481S</sup> TMD8 cells

Next, we compared the potency of BTK PROTACs in TMD8 cells (Table 5 and Table S2), a BTK dependent diffuse large B-cell lymphoma (DLBCL) cell line. In BTK<sup>WT</sup> TMD8 cells, **4f**, **4g**, **6d** and **6e** have moderate to potent potency for inhibiting cell growth, and these BTK PROTACs are more potent than the BTK inhibitor ARQ531. **6d** and **6e** are about 2-folds more potent than **4f** and **4g**. Additionally, **6d** and **6e** can inhibit not only BTK<sup>WT</sup> TMD8 cell growth but also BTK<sup>C481S</sup> TMD8 cell growth with IC<sub>50</sub> of 290.1 nM and 253.5 nM, respectively, which are comparable with ARQ531. It is interesting to note that **4f** and **4g** dropped their inhibition potency in BTK<sup>C481S</sup> TMD8 cells, which might be due to the weak BTK<sup>C481S</sup> degradation. Overall, the cell proliferation inhibition results are essentially consistent with the degradation potency.

### 2.4. The membrane permeability and plasma stability

Though the designed PROTACs are proved to degrade WT and mutant BTK, the high molecular weight and multiple hydrogen

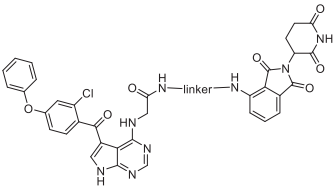
bond donors (HBDs) and acceptors (HBAs) of PROTACs always limit their physicochemical properties, such as membrane permeability and stability [30–32]. We measured the *in vitro* plasma half-life of the warhead-A and warhead-B based PROTACs. **4f** and **6e** showed good stability in human plasma with the T<sub>1/2</sub> of 320.2 min and 212.8 min respectively (Table 6). Next, PROTAC **6e** with potent BTK<sup>C481S</sup> degradation and cell proliferation inhibition was selected to measure the membrane permeability. As shown in Table 7, PROTAC **6e** has a moderate membrane permeability with the measured Caco-2 permeability P<sub>app(B-A)</sub> = 7.5 × 10<sup>-6</sup> cm/s, which is above the standard for “modest” permeability (P<sub>app</sub> = 1.0 × 10<sup>-6</sup> cm/s). These membrane permeability and plasma stability testing results indicated that warhead-B based PROTAC as **6e** is potent with some acceptable physicochemical properties.

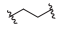
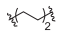
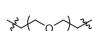





## 3. Conclusions

In summary, we discovered a series of novel BTK PROTACs based on the reversible non-covalent BTK inhibitor ARQ531. Both the weak binding warhead-A based PROTACs and strong binding warhead-B based PROTACs could degrade BTK<sup>WT</sup> and BTK<sup>C481S</sup>, but



**Table 2**  
BTK inhibition and degradation of warhead-A based PROTACs with different linkers.



Compd.	Linker	Linker atoms	BTK Inhibition <sup>1</sup> (%)		IC <sub>50</sub> (BTK <sup>WT</sup> , nM)	BTK degradation <sup>1,2</sup> (%) @100 nM	DC <sub>50</sub> (nM)	D <sub>max</sub> %
			@50 nM	@500 nM				
<b>ARQ531</b>			89.5 ± 0.5	98.7 ± 0.1	8.2 ± 0.7	7.5 ± 1.5	ND <sup>3</sup>	ND <sup>3</sup>
<b>4a</b>		2	2.4 ± 1.3	10.9 ± 0.8	ND <sup>3</sup>	ND <sup>3</sup>	ND <sup>3</sup>	ND <sup>3</sup>
<b>4b</b>		4	1.8 ± 2.4	9.3 ± 2.2	ND <sup>3</sup>	24.9 ± 1.3	ND <sup>3</sup>	ND <sup>3</sup>
<b>4c</b>		8	7.5 ± 3.5	21.5 ± 2.1	3775.0 ± 267.3	33.0 ± 0.8	ND <sup>3</sup>	ND <sup>3</sup>
<b>4d</b>		11	8.6 ± 0.3	21.6 ± 1.4	1931.5 ± 102.5	56.2 ± 3.7	28.5 ± 3.7	67.1 ± 3.3
<b>4e</b>		14	5.6 ± 3.5	35.6 ± 1.7	2203.5 ± 36.1	55.6 ± 2.9	9.4 ± 0.8	66.5 ± 2.1
<b>4f</b>		17	5.9 ± 4.6	35.5 ± 0.5	1209.5 ± 36.1	64.2 ± 1.1	8.1 ± 0.4	72.4 ± 4.5
<b>4g</b>		20	10.0 ± 4.8	42.5 ± 0.6	1390.5 ± 205.8	78.7 ± 0.7	8.3 ± 0.3	92.4 ± 3.0
<b>4h</b>		23	7.0 ± 0.8	39.0 ± 0.8	ND <sup>3</sup>	14.7 ± 3.2	ND <sup>3</sup>	ND <sup>3</sup>

<sup>1</sup> BTK IC<sub>50</sub> and DC<sub>50</sub> values are the average of at least two determinations.

<sup>2</sup> The BTK<sup>WT</sup> degradation in JeKo-1 cells.

<sup>3</sup> ND: not determined.

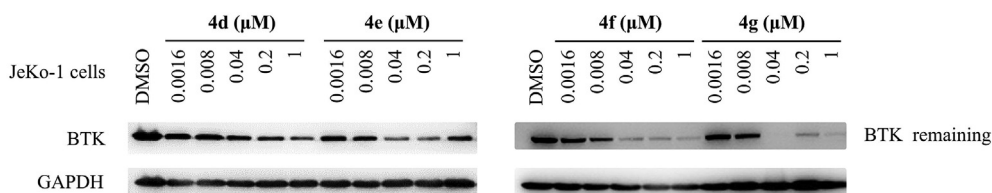


**Fig. 2.** Examination of dose-dependent BTK degradation by **4d**, **4e**, **4f** and **4g** in JeKo-1 cells, with glyceraldehyde-3-phosphate dehydrogenase (GAPDH) used as the loading control.

warhead-B based PROTACs are more potent on BTK<sup>C481S</sup> TMD8 cell proliferation inhibition. Within the warhead-B PROTACs, **6e** is the most potent PROTAC with strong BTK<sup>WT</sup> and BTK<sup>C481S</sup> degradation, effectively BTK<sup>WT</sup> and BTK<sup>C481S</sup> TMD8 cell proliferation inhibition, moderate membrane permeability and good plasma stability. These data provided a basis for developing new and potent reversible non-covalent PROTAC-based therapeutic molecules.

## 4. Experimental section

### 4.1. General synthetic procedures

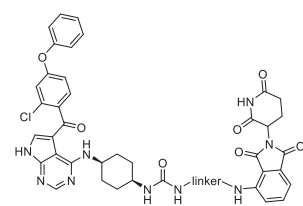
All the reagents used were commercially available and were used as received unless otherwise indicated. Microwave reaction was conducted with a Biotage Initiator<sup>TM</sup> microwave synthesizer. NMR data were recorded with a Bruker 400 MHz NMR system. Chemical shifts ( $\delta$ ) are expressed in parts per million (ppm) relative to tetramethylsilane (TMS) as an internal standard. Mass spectra were measured on an Agilent 1100 series LC/MSD 1947d spectrometer (Agilent Technologies, Inc., Santa Clara, CA, USA). High-resolution mass spectra (HRMS) were obtained on an AB SCIEX TripleTOF 5600+ mass spectrometer (AB SCIEX, LLC., Redwood City,

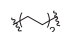




CA, USA). The contents of compounds for biological evaluation were examined with an Agilent 1260 Infinity LC system (Agilent Technologies, Inc., Santa Clara, CA, USA) with methanol/water (40/60 to 95/5) as the eluent. Unless specified, the purity of target compounds was >95%, which was considered to be pure enough for biological assays. <sup>1</sup>H NMR, <sup>13</sup>C NMR and HRMS are detailed in the Supporting Information section.

### 4.2. General procedure for synthesis of compounds **A3a-A3b**, **A4a-A4f**

**Step A:** A solution of 3-aminopiperidine-2,6-dione hydrochloride (2.20 g, 13.24 mmol) and 4-fluoroisobenzofuran-1,3-dione (**A1**) (2.00 g, 12.04 mmol) in HOAc (30 mL), and then the NaOAc (1.20 g, 14.63 mmol) was added. The mixture was stirred at 140 °C for 3 h. The solvents were evaporated under reduced pressure, then H<sub>2</sub>O (30 mL) was added into the residue, the mixture was stirred at room temperature for 0.5 h. After filtration and evaporation, the crude **A2** (2.90 g, 88% yield) was obtained as off-white solid, which was used for the next step without further purification. <sup>1</sup>H NMR (400 MHz, DMSO-*d*<sub>6</sub>)  $\delta$  11.19 (s, 1H), 7.96 (s, 1H), 7.79 (dd, *J* = 16.1, 8.0 Hz, 2H), 5.18 (d, *J* = 12.2 Hz, 1H), 2.89 (d, *J* = 15.4 Hz, 1H), 2.62 (d,

**Table 3**  
BTK inhibition and degradation of warhead-B based PROTACs with different linkers.



Compd.	Linker	Linker atoms	BTK inhibition <sup>1</sup> (%)		IC <sub>50</sub> (BTK <sup>WT</sup> , nM)	BTK degradation <sup>1</sup> (%) @100 nM	DC <sub>50</sub> (nM)	D <sub>max</sub> %
			@50 nM	@500 nM				
<b>ARQ531</b>								
<b>6a</b>		4	89.5 ± 0.5 75.0 ± 3.1	98.7 ± 0.1 96.2 ± 0.6	8.2 ± 0.7 23.0 ± 3.7	7.5 ± 1.5 6.8 ± 0.4	ND <sup>2</sup> ND <sup>2</sup>	ND <sup>2</sup> ND <sup>2</sup>
<b>6b</b>		8	82.1 ± 1.1	97.4 ± 1.0	15.5 ± 1.2	22.8 ± 1.1	ND <sup>2</sup>	ND <sup>2</sup>
<b>6c</b>		11	73.5 ± 0.3	95.2 ± 0.0	22.3 ± 1.0	44.1 ± 2.8	32.3 ± 8.0	76.9 ± 0.7
<b>6d</b>		14	32.6 ± 3.3	74.9 ± 4.7	46.9 ± 1.4	88.8 ± 0.4	12.1 ± 2.7	78.0 ± 4.6
<b>6e</b>		17	58.4 ± 0.9	90.0 ± 0.0	56.4 ± 6.9	93.7 ± 1.9	41.9 ± 5.3	93.0 ± 1.6

<sup>1</sup> BTK IC<sub>50</sub> and DC<sub>50</sub> values are the average of at least two determinations.

<sup>2</sup> ND: not determined.

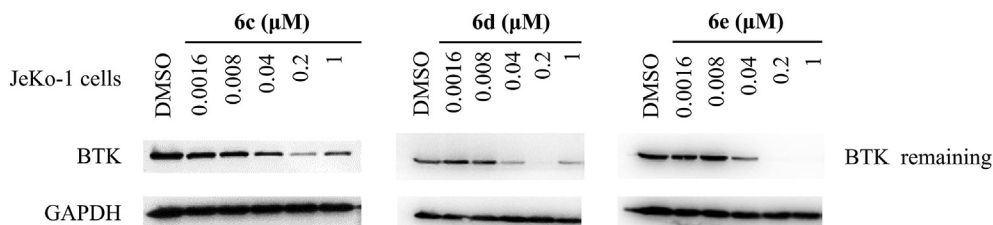


**Fig. 3.** Examination of dose-dependent BTK degradation by **6c**, **6d** and **6e** in JeKo-1 cells, with GAPDH used as the loading control.

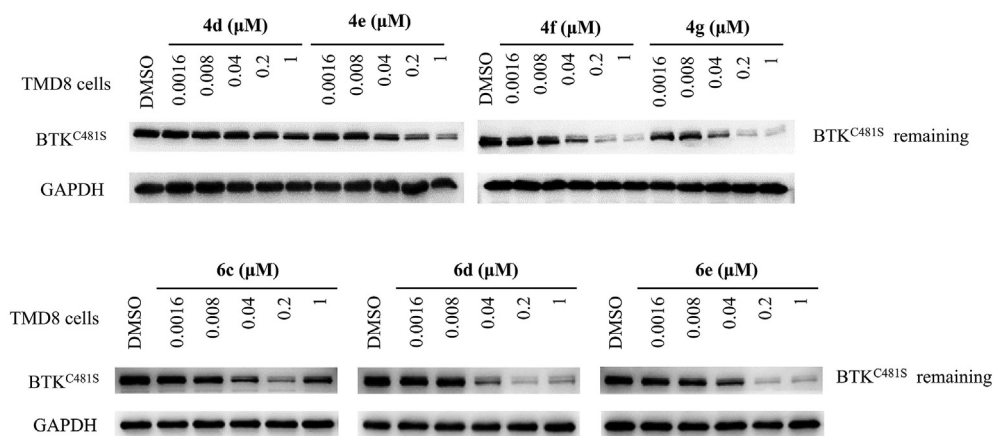


**Fig. 4.** Examination of dose-dependent BTK<sup>C481S</sup> degradation by **4e**, **4f**, **4g**, **6c**, **6d** and **6e** in TMD8 cells, with GAPDH used as the loading control.

$J = 17.9$  Hz, 1H), 2.09 (s, 1H). LC-MS (ESI)  $m/z$ : calcd C<sub>13</sub>H<sub>9</sub>FN<sub>2</sub>O<sub>4</sub> [M+H]<sup>+</sup>: 276.05; found 276.90.

**Step B:** To a solution of 2-(2,6-Dioxopiperidin-3-yl)-4-fluoroisindoline-1,3-dione (**A2**) (0.20 g, 0.72 mmol) and *tert*-butyl(2-aminoethyl)carbamate (0.13 g, 0.81 mmol) in DMF (15 ml) was added DIPEA (0.19 g, 1.44 mmol). The mixture was placed in a microwave reactor and stirred at 110 °C for 2 h. The reaction mixture was diluted with ethyl acetate (30 mL) and H<sub>2</sub>O (20 mL).

The separated aqueous phase was extracted with ethyl acetate (3 × 30 mL), and the combined organic layer was washed with water and saturated brine, dried over anhydrous Na<sub>2</sub>SO<sub>4</sub>. After filtration and evaporation, the residue was subjected to flash column chromatography with PE/EA (1/2) to furnish *tert*-butyl (2-((2-(2,6-dioxopiperidin-3-yl)-1,3-dioxoisindolin-4-yl)amino)ethyl) carbamate (0.13 g, 44% yield) as a yellow solid. <sup>1</sup>H NMR (400 MHz, DMSO-*d*<sub>6</sub>)  $\delta$  11.12 (s, 1H), 7.58 (s, 1H), 7.15 (d,  $J = 8.3$  Hz, 1H), 7.04 (s,

**Table 4**  
BTK<sup>C481S</sup> degradation of the designed reversible non-covalent PROTACs.

Compd.	BTK <sup>C481S</sup> degradation DC <sub>50</sub> (nM) <sup>1</sup>	D <sub>max</sub> %
<b>4e</b>	52.7 ± 11.9	68.6 ± 1.7
<b>4f</b>	80.4 ± 25.2	88.4 ± 13.0
<b>4g</b>	52.3 ± 11.3	84.8 ± 1.6
<b>6c</b>	30.1 ± 4.8	84.3 ± 3.1
<b>6d</b>	37.9 ± 0.4	83.5 ± 0.5
<b>6e</b>	42.9 ± 1.6	90.7 ± 5.1

<sup>1</sup> BTK<sup>C481S</sup> DC<sub>50</sub> values are the average of at least two determinations**Table 5**  
The cell proliferation inhibition potency of BTK PROTACs in TMD8 cells and BTK<sup>C481S</sup> TMD8 cells.

Compd.	BTK <sup>WT</sup> TMD8 Cells IC <sub>50</sub> (nM) <sup>1</sup>	BTK <sup>C481S</sup> TMD8 Cells IC <sub>50</sub> (nM) <sup>1</sup>
<b>4f</b>	63.3 ± 2.9	1689.3 ± 11.3
<b>4g</b>	104.5 ± 3.2	750.0 ± 56.6
<b>6d</b>	39.5 ± 1.1	290.1 ± 29.2
<b>6e</b>	45.7 ± 2.8	253.5 ± 8.7
<b>ARQ531</b>	188.6 ± 12.8	229.2 ± 18.2

<sup>1</sup> BTK<sup>WT</sup> TMD8 cells and BTK<sup>C481S</sup> TMD8 cells DC<sub>50</sub> values are the average of at least two determinations.**Table 6**  
The plasma stability of **4f** and **6e**.

Compd.	Species	T <sub>1/2</sub> (min) <sup>1</sup>
<b>4f</b>	human	320.2
<b>6e</b>		212.8

<sup>1</sup> Duplicates were performed (n = 2).

2H), 6.73 (s, 1H), 5.06 (d, *J* = 7.5 Hz, 1H), 3.12 (s, 2H), 2.89 (s, 1H), 2.59 (d, *J* = 18.4 Hz, 1H), 2.01 (s, 1H), 1.36 (s, 9H), 1.25 (s, 1H), 1.16 (d, *J* = 6.1 Hz, 2H). LC-MS (ESI) *m/z*: calcd C<sub>20</sub>H<sub>24</sub>N<sub>4</sub>O<sub>6</sub> [M+H]<sup>+</sup>: 416.17; found 316.80.

Step C: A solution of *tert*-butyl (2-((2-(2,6-dioxopiperidin-3-yl)-1,3-dioxoisindolin-4-yl)amino)ethyl)carbamate in 1:1 TFA/DCM was stirred at room temperature for 1 h. The solvents were evaporated under reduced pressure to give the corresponding deprotected intermediate **A3a** (TFA salt) that was used in the following reactions without further purification (95% yield).

Following the procedures used to prepare compound **A3a**, compounds **A3b** and **A4a–A4f** with different chain lengths were obtained by the same methods.

#### 4.3. General procedure for synthesis of compounds **2**, **3**, **4**

Step A: A solution of phenol (0.90 g, 9.6 mmol) and NaH (0.51 g, 12.8 mmol) in DMF (30 mL) was stirred at room temperature for 10 min under N<sub>2</sub>. Then, 2-chloro-4-fluorobenzonitrile (**B1**) (1.00 g, 6.4 mmol) was added into the solution. The reaction mixture was stirred at room temperature for 1 h. After the reaction, the mixture was diluted with water (20 mL) and extracted with ethyl acetate (3 × 30 mL). The combined organic layer was washed with brine solution, dried over Na<sub>2</sub>SO<sub>4</sub> and concentrated. The crude product was purified by silica chromatography (200–300 mesh) using a

**Table 7**  
The membrane permeability of **6e** in Caco-2 cell lines.

Compd.	A-B permeability (P <sub>app</sub> × 10 <sup>-6</sup> cm/s) <sup>1</sup>	B-A permeability (P <sub>app</sub> × 10 <sup>-6</sup> cm/s) <sup>1</sup>	Efflux ratio (P <sub>app(B-A)</sub> /P <sub>app(A-B)</sub> )
<b>6e</b>	<5.3	7.5	>1.4

<sup>1</sup> Duplicates were performed (n = 2).

solvent gradient of (100% petroleum ether) to give **B2** (1.41 g, 96% yield) as a white solid. <sup>1</sup>H NMR (400 MHz, DMSO-*d*<sub>6</sub>) δ 7.95 (dd, *J* = 7.3, 4.0 Hz, 1H), 7.50 (d, *J* = 6.0 Hz, 2H), 7.30 (s, 1H), 7.28–7.20 (m, 3H), 7.11–6.92 (m, 1H). LC-MS (ESI) *m/z*: calcd C<sub>13</sub>H<sub>8</sub>ClNO [M+H]<sup>+</sup>: 229.03; found 229.90.

Step B: To a solution of 5 M sodium hydroxide aqueous solution (18 mL) in absolute ethanol (12 mL) was added 2-chloro-4-phenoxybenzonitrile (**B2**) (1.41 g, 6.1 mmol). The mixture was stirred at 85 °C overnight under N<sub>2</sub> atmosphere. After cooling to room temperature, the reaction solution was added concentrated hydrochloric acid to pH = 3. The reaction mixture was extracted with ethyl acetate (3 × 30 mL). The combined organic layer was washed with brine solution, dried over Na<sub>2</sub>SO<sub>4</sub> and concentrated to give **B3** (1.43 g, 90.0% yield) as a white solid. It was used in the next step without any further purification. <sup>1</sup>H NMR (400 MHz, DMSO-*d*<sub>6</sub>) δ 13.25 (s, 1H), 7.98–7.83 (m, 1H), 7.54–7.43 (m, 2H), 7.28 (d, *J* = 6.7 Hz, 1H), 7.16 (d, *J* = 7.8 Hz, 2H), 7.12–7.04 (m, 1H), 7.01–6.92 (m, 1H). LC-MS (ESI) *m/z*: calcd C<sub>13</sub>H<sub>9</sub>ClO<sub>3</sub> [M+H]<sup>+</sup>: 248.02; found 248.90.

Step C: To a solution of 2-chloro-4-phenoxybenzoic acid (**B3**) (1.43 g, 5.8 mmol) and CH<sub>3</sub>I (0.98 g, 6.9 mmol) in DMF (30 mL) was added K<sub>2</sub>CO<sub>3</sub> (1.59 g, 11.5 mmol). The mixture was stirred at room temperature for 1 h. The reaction mixture was diluted with water (20 mL) and extracted with ethyl acetate (3 × 30 mL). The combined organic layer was washed with brine solution, dried over Na<sub>2</sub>SO<sub>4</sub> and concentrated. The crude product was purified by silica chromatography (200–300 mesh) using a solvent gradient of (10/1 to 4/1 petroleum ether/ethyl acetate) to give **B4** (1.34 g, 88.4% yield) as a white solid. <sup>1</sup>H NMR (400 MHz, DMSO-*d*<sub>6</sub>) δ 7.95–7.84 (m, 1H), 7.48 (s, 2H), 7.29 (s, 1H), 7.17 (s, 2H), 7.14–7.08 (m, 1H), 6.98 (dd, *J* = 6.3, 2.3 Hz, 1H), 3.83 (dd, *J* = 6.3, 2.3 Hz, 3H). LC-MS (ESI) *m/z*: calcd C<sub>14</sub>H<sub>11</sub>ClO<sub>3</sub> [M+H]<sup>+</sup>: 262.04; found 262.80.

Step D: To a solution of 5-bromo-4-chloro-7H-pyrrolo[2,3-d]pyrimidine (0.84 g, 3.6 mmol) in THF (20 mL) was added *n*-BuLi (2.5 M solution in hexanes 3.4 mL) under N<sub>2</sub>. The mixture was stirred at –78 °C for 1 h. Then methyl-2-chloro-4-phenoxybenzoate (**B4**) (1.00 g, 3.8 mmol) in THF (5 mL) was added into the solution, and the mixture was stirred at –78 °C for 1 h. After reaction, the mixture was quenched with 1 N HCl (20 mL) and extracted with ethyl acetate (3 × 30 mL). The combined organic layer was washed with brine solution, dried over Na<sub>2</sub>SO<sub>4</sub> and concentrated. The crude product was purified by silica chromatography (200–300 mesh) using a solvent gradient of (10/1 to 2/1 petroleum ether/ethyl acetate) to give **B5** (0.35 g, 23.3% yield) as a white solid. <sup>1</sup>H NMR (400 MHz, DMSO-*d*<sub>6</sub>) δ 13.43 (s, 1H), 8.75 (s, 1H), 8.14 (s, 1H), 7.59 (d, *J* = 8.5 Hz, 1H), 7.48 (s, 2H), 7.26 (s, 1H), 7.18 (s, 3H), 7.01 (d, *J* = 8.5 Hz, 1H). LC-MS (ESI) *m/z*: calcd C<sub>19</sub>H<sub>11</sub>Cl<sub>2</sub>N<sub>3</sub>O<sub>2</sub> [M+H]<sup>+</sup>: 383.02; found 383.90.

To a solution of (2-chloro-4-phenoxyphenyl)(4-chloro-7H-pyrrolo[2,3-d]pyrimidin-5-yl)methanone **B5** (0.20 g, 0.52 mmol) and *tert*-butyl glycinate (0.08 g, 0.57 mmol) in IPA (10 mL) was added DIPEA (0.20 mg, 1.56 mmol) under N<sub>2</sub>. The mixture solution was heated to reflux for 3 h. The solvent was evaporated in vacuo and the resulting solid was diluted with H<sub>2</sub>O (10 mL). The mixture solution was stirred at room temperature for 0.5 h and then it was filtered. The crude product was purified by silica chromatography (200–300 mesh) using a solvent gradient of (10/1 to 1/3 petroleum



ether/ethyl acetate) to give *tert*-butyl (5-(2-chloro-4-phenoxybenzoyl)-7H-pyrrolo[2,3-d]pyrimidin-4-yl)glycinate (0.13 g, 54% yield) as a white solid.

**(5-(2-Chloro-4-phenoxybenzoyl)-7H-pyrrolo[2,3-d]pyrimidin-4-yl)glycine(2).** A solution of *tert*-butyl (5-(2-chloro-4-phenoxybenzoyl)-7H-pyrrolo[2,3-d]pyrimidin-4-yl)glycinate in 1:1 TFA/DCM was stirred at room temperature for 1 h. The solvents were evaporated under reduced pressure to give compound **2** (TFA salt) that was used in the following reactions without further purification (95% yield). <sup>1</sup>H NMR (400 MHz, DMSO-*d*<sub>6</sub>) δ 12.76 (s, 2H), 8.94 (t, *J* = 5.6 Hz, 1H), 8.26 (s, 1H), 7.66 (s, 1H), 7.59 (d, *J* = 8.4 Hz, 1H), 7.48 (t, *J* = 7.9 Hz, 2H), 7.25 (t, *J* = 7.4 Hz, 1H), 7.22–7.15 (m, 3H), 7.03 (dd, *J* = 8.4, 2.2 Hz, 1H), 4.29 (d, *J* = 5.6 Hz, 2H). <sup>13</sup>C NMR (101 MHz, DMSO-*d*<sub>6</sub>) δ 189.31, 171.59, 158.61, 156.40, 155.24, 153.82, 152.69, 136.00, 133.43, 131.21, 130.76, 130.33, 124.67, 119.64, 119.12, 116.32, 100.55, 42.19. HRMS (ESI) *m/z*: calcd C<sub>21</sub>H<sub>15</sub>ClN<sub>4</sub>O<sub>4</sub> [M+H]<sup>+</sup>: 423.0855; found 423.0874.

**Ethyl (5-(2-Chloro-4-phenoxybenzoyl)-7H-pyrrolo[2,3-d]pyrimidin-4-yl)glycinate(3).** To a solution of (2-chloro-4-phenoxyphenyl)(4-chloro-7H-pyrrolo[2,3-d]pyrimidin-5-yl)methanone **B5** (0.20 g, 0.52 mmol) and ethyl glycinate (0.08 g, 0.57 mmol) in IPA (10 mL) was added DIPEA (0.20 mg, 1.56 mmol) under N<sub>2</sub>. The mixture was heated to reflux for 3 h. The solvent was evaporated in vacuo and the resulting solid was diluted with H<sub>2</sub>O (10 mL). The mixture solution was stirred at room temperature for 0.5 h and filtered. The crude product was purified by silica chromatography (200–300 mesh) using a solvent gradient of (10/1 to 1/3 petroleum ether/ethyl acetate) to give compound **3** in 54.0% yield as a white solid. <sup>1</sup>H NMR (400 MHz, DMSO-*d*<sub>6</sub>) δ 12.83 (s, 1H), 8.97 (s, 1H), 8.26 (s, 1H), 7.69 (s, 1H), 7.60 (d, *J* = 7.8 Hz, 1H), 7.49 (t, *J* = 6.8 Hz, 2H), 7.27 (d, *J* = 6.7 Hz, 1H), 7.20 (d, *J* = 6.0 Hz, 3H), 7.04 (d, *J* = 8.2 Hz, 1H), 4.37 (d, *J* = 3.7 Hz, 2H), 4.15 (d, *J* = 6.7 Hz, 2H), 1.22 (t, *J* = 6.0 Hz, 3H). <sup>13</sup>C NMR (101 MHz, DMSO-*d*<sub>6</sub>) δ 194.60, 175.46, 163.91, 161.68, 160.50, 159.04, 157.99, 141.34, 138.65, 136.49, 136.02, 135.59, 129.94, 124.91, 124.37, 121.55, 105.85, 65.69, 19.33. HRMS (ESI) *m/z*: calcd C<sub>23</sub>H<sub>19</sub>ClN<sub>4</sub>O<sub>4</sub> [M+H]<sup>+</sup>: 451.1168; found 451.1172.

**2-((5-(2-Chloro-4-phenoxybenzoyl)-7H-pyrrolo[2,3-d]pyrimidin-4-yl)amino)-N-ethylacetamide(4).** To a solution of compound **2** (0.10 g, 0.24 mmol), DIPEA (5.0 equiv) and ethylamine (1.2 equiv) in DMF (10 mL) was added HATU (1.2 equiv). The mixture was stirred at room temperature for 2 h. The reaction mixture was quenched with H<sub>2</sub>O and extracted with ethyl acetate. The organic layer was separated, washed with brine, dried, and evaporated. The final compound **4** was obtained by flash column chromatography (DCM/MeOH = 4/1) in 45.4% yield. <sup>1</sup>H NMR (400 MHz, DMSO-*d*<sub>6</sub>) δ 12.75 (s, 1H), 8.96 (t, *J* = 5.3 Hz, 1H), 8.25 (s, 1H), 8.08 (s, 1H), 7.64 (s, 1H), 7.57 (d, *J* = 8.5 Hz, 1H), 7.52–7.45 (m, 2H), 7.26 (t, *J* = 7.4 Hz, 1H), 7.23–7.18 (m, 3H), 7.04 (dd, *J* = 8.4, 2.4 Hz, 1H), 4.17 (d, *J* = 5.4 Hz, 2H), 3.24–3.02 (m, 2H), 1.04 (t, *J* = 7.2 Hz, 3H). <sup>13</sup>C NMR (101 MHz, DMSO-*d*<sub>6</sub>) δ 189.11, 168.43, 158.58, 156.42, 155.22, 153.87, 152.62, 135.75, 133.49, 131.21, 130.75, 130.34, 124.68, 119.66, 119.10, 116.52, 116.18, 100.60, 43.51, 33.39, 14.74. HRMS (ESI) *m/z*: calcd C<sub>23</sub>H<sub>20</sub>ClN<sub>5</sub>O<sub>3</sub> [M+H]<sup>+</sup>: 450.1327; found 450.1326.

#### 4.4. General procedure for synthesis of compounds 4a–4h

**2-((5-(2-Chloro-4-phenoxybenzoyl)-7H-pyrrolo[2,3-d]pyrimidin-4-yl)amino)-N-(2-((2-(2,6-dioxopiperidin-3-yl)-1,3-dioxoisindolin-4-yl)amino)ethoxy)ethyl)acetamide (4a).** To a solution of compound **2** (0.13 g, 0.3 mmol), DIPEA (5 equiv) and **A3a** (1.1 equiv) in DMF (5 mL) was added HATU (1.2 equiv). The mixture was stirred at room temperature for 2 h. The reaction mixture was quenched with H<sub>2</sub>O and extracted with ethyl acetate. The organic layer was separated, washed with brine, dried, and evaporated. The final

compound **4a** was obtained by flash column chromatography (DCM/MeOH = 4/1) in 13.0% yield. <sup>1</sup>H NMR (400 MHz, DMSO-*d*<sub>6</sub>) δ 12.76 (s, 1H), 11.11 (s, 1H), 8.98 (t, *J* = 5.4 Hz, 1H), 8.34 (t, *J* = 5.6 Hz, 1H), 8.24 (s, 1H), 7.66 (s, 1H), 7.59 (dd, *J* = 12.1, 5.5 Hz, 2H), 7.53–7.46 (m, 2H), 7.32–7.25 (m, 1H), 7.25–7.19 (m, 4H), 7.08–7.02 (m, 2H), 6.80 (t, *J* = 6.1 Hz, 1H), 5.07 (dd, *J* = 12.9, 5.4 Hz, 1H), 4.20 (d, *J* = 5.4 Hz, 2H), 3.43 (dt, *J* = 14.9, 7.5 Hz, 2H), 3.33 (d, *J* = 5.9 Hz, 2H), 2.89–2.80 (m, 1H), 2.64–2.54 (m, 2H), 2.10–1.96 (m, 1H). <sup>13</sup>C NMR (101 MHz, DMSO-*d*<sub>6</sub>) δ 189.14, 172.78, 170.07, 169.47, 168.66, 167.27, 158.60, 156.46, 155.24, 152.67, 146.30, 136.18, 133.49, 132.20, 131.22, 130.74, 130.34, 124.68, 119.66, 119.12, 117.11, 116.51, 116.21, 110.53, 109.26, 100.65, 60.69, 48.49, 43.54, 41.29, 38.11, 30.95, 29.17, 22.12. HRMS (ESI) *m/z*: calcd C<sub>36</sub>H<sub>29</sub>ClN<sub>8</sub>O<sub>7</sub> [M+H]<sup>+</sup>: 721.1920; found 721.1929.

Following the procedures used to prepare compound **4a**, compounds **4b–4h** with different chain lengths were obtained by the same methods.

**2-((5-(2-Chloro-4-phenoxybenzoyl)-7H-pyrrolo[2,3-d]pyrimidin-4-yl)amino)-N-(4-((2-(2,6-dioxopiperidin-3-yl)-1,3-dioxoisindolin-4-yl)amino)butyl)acetamide (4b).** Yield 21.7%. <sup>1</sup>H NMR (400 MHz, DMSO-*d*<sub>6</sub>) δ 12.75 (s, 1H), 11.11 (s, 1H), 8.98 (t, *J* = 5.4 Hz, 1H), 8.24 (s, 1H), 8.11 (t, *J* = 5.7 Hz, 1H), 7.65 (s, 1H), 7.57 (t, *J* = 7.6 Hz, 2H), 7.53–7.47 (m, 2H), 7.31–7.24 (m, 1H), 7.24–7.19 (m, 3H), 7.12 (d, *J* = 8.6 Hz, 1H), 7.08–6.99 (m, 2H), 6.58 (t, *J* = 5.9 Hz, 1H), 5.07 (dd, *J* = 12.9, 5.4 Hz, 1H), 4.19 (d, *J* = 5.4 Hz, 2H), 3.32 (d, *J* = 6.6 Hz, 2H), 3.17 (q, *J* = 6.3 Hz, 2H), 2.89–2.80 (m, 1H), 2.61 (d, *J* = 2.6 Hz, 1H), 2.60–2.54 (m, 1H), 2.09–2.00 (m, 1H), 1.60 (dd, *J* = 14.3, 7.2 Hz, 2H), 1.53 (dd, *J* = 13.9, 6.8 Hz, 2H). <sup>13</sup>C NMR (101 MHz, DMSO-*d*<sub>6</sub>) δ 189.10, 172.79, 170.08, 168.80, 167.28, 158.58, 156.44, 155.24, 153.83, 152.65, 146.36, 136.21, 135.74, 133.51, 132.16, 131.22, 130.73, 130.34, 124.68, 119.65, 119.11, 117.21, 116.51, 116.19, 110.31, 108.96, 100.64, 48.50, 43.58, 41.50, 38.13, 30.95, 26.53, 26.11, 22.12. HRMS (ESI) *m/z*: calcd C<sub>38</sub>H<sub>33</sub>ClN<sub>8</sub>O<sub>7</sub> [M+H]<sup>+</sup>: 749.2234; found 749.2257.

**2-((5-(2-Chloro-4-phenoxybenzoyl)-7H-pyrrolo[2,3-d]pyrimidin-4-yl)amino)-N-(2-(2-(2-((2-(2,6-dioxopiperidin-3-yl)-1,3-dioxoisindolin-4-yl)amino)ethoxy)ethoxy)ethyl)acetamide (4c).** Yield 20.3%. <sup>1</sup>H NMR (400 MHz, DMSO-*d*<sub>6</sub>) δ 12.75 (s, 1H), 11.11 (s, 1H), 8.97 (t, *J* = 5.4 Hz, 1H), 8.24 (d, *J* = 5.7 Hz, 1H), 8.13 (t, *J* = 5.6 Hz, 1H), 7.64 (s, 1H), 7.58 (dt, *J* = 8.4, 3.6 Hz, 2H), 7.53–7.47 (m, 2H), 7.31–7.24 (m, 1H), 7.24–7.18 (m, 3H), 7.14 (d, *J* = 8.6 Hz, 1H), 7.08–7.01 (m, 2H), 6.62 (t, *J* = 5.7 Hz, 1H), 5.07 (dd, *J* = 12.9, 5.4 Hz, 1H), 4.20 (d, *J* = 5.3 Hz, 2H), 3.63 (t, *J* = 5.4 Hz, 2H), 3.57 (td, *J* = 4.8, 2.7 Hz, 4H), 3.47 (dd, *J* = 11.6, 5.6 Hz, 4H), 3.28 (dd, *J* = 11.4, 5.7 Hz, 2H), 2.89–2.80 (m, 1H), 2.64–2.53 (m, 2H), 2.03–1.95 (m, 1H). <sup>13</sup>C NMR (101 MHz, DMSO-*d*<sub>6</sub>) δ 189.09, 172.77, 170.07, 168.93, 167.26, 158.58, 156.41, 155.23, 153.83, 152.69, 146.35, 136.17, 135.80, 133.50, 132.05, 131.22, 130.73, 130.34, 124.67, 119.65, 119.10, 117.37, 116.50, 116.19, 110.62, 109.20, 100.62, 69.63, 69.26, 68.95, 48.52, 43.51, 41.65, 38.60, 30.94, 22.10. HRMS (ESI) *m/z*: calcd C<sub>40</sub>H<sub>37</sub>ClN<sub>8</sub>O<sub>9</sub> [M+H]<sup>+</sup>: 809.2445; found 809.2436.

**2-((5-(2-Chloro-4-phenoxybenzoyl)-7H-pyrrolo[2,3-d]pyrimidin-4-yl)amino)-N-(2-(2-(2-(2-((2-(2,6-dioxopiperidin-3-yl)-1,3-dioxoisindolin-4-yl)amino)ethoxy)ethoxy)ethoxy)ethyl)acetamide (4d).** Yield 15.7%. <sup>1</sup>H NMR (400 MHz, DMSO-*d*<sub>6</sub>) δ 12.73 (s, 1H), 11.10 (s, 1H), 8.95 (t, *J* = 5.4 Hz, 1H), 8.24 (s, 1H), 8.12 (t, *J* = 5.6 Hz, 1H), 7.63 (s, 1H), 7.56 (dt, *J* = 8.4, 3.6 Hz, 2H), 7.51–7.45 (m, 2H), 7.26 (t, *J* = 7.4 Hz, 1H), 7.22–7.17 (m, 3H), 7.13 (d, *J* = 8.6 Hz, 1H), 7.06–7.00 (m, 2H), 6.60 (t, *J* = 5.7 Hz, 1H), 5.06 (dd, *J* = 12.9, 5.4 Hz, 1H), 4.19 (d, *J* = 5.3 Hz, 2H), 3.61 (t, *J* = 5.4 Hz, 2H), 3.54–3.45 (m, 6H), 3.45 (dd, *J* = 11.6, 5.6 Hz, 6H), 3.26 (dd, *J* = 11.4, 5.7 Hz, 2H), 2.88–2.80 (m, 1H), 2.63–2.52 (m, 2H), 2.07–1.95 (m, 1H). <sup>13</sup>C NMR (101 MHz, DMSO-*d*<sub>6</sub>) δ 189.08, 172.78, 170.05, 168.93, 167.26, 158.58, 156.42, 155.23, 153.83, 152.70, 146.35, 136.17, 135.82, 133.51, 132.04, 131.21, 130.73, 130.33, 124.67, 119.65, 119.10, 117.39, 116.50, 116.19, 110.62, 109.19, 100.62, 69.67, 68.91, 48.52, 43.50, 41.65, 38.60, 30.94,

22.11. HRMS (ESI)  $m/z$ : calcd  $C_{42}H_{41}ClN_8O_{10}$   $[M+H]^+$ : 853.2707; found 853.2734.

**2-((5-(2-Chloro-4-phenoxybenzoyl)-7H-pyrrolo[2,3-d]pyrimidin-4-yl)amino)-N-(14-((2-(2,6-dioxopiperidin-3-yl)-1,3-dioxoisindolin-4-yl)amino)-3,6,9,12-tetraoxatetradecyl)acetamide (4e).** Yield 12.3%.  $^1H$  NMR (400 MHz, DMSO- $d_6$ )  $\delta$  12.78 (s, 1H), 11.10 (s, 1H), 9.01 (t,  $J$  = 4.9 Hz, 1H), 8.25 (s, 1H), 8.14 (t,  $J$  = 5.6 Hz, 1H), 7.64 (s, 1H), 7.56 (dt,  $J$  = 8.4, 3.6 Hz, 2H), 7.52-7.44 (m, 2H), 7.29-7.22 (m, 1H), 7.21-7.16 (m, 3H), 7.13 (d,  $J$  = 8.6 Hz, 1H), 7.06-6.99 (m, 2H), 6.60 (t,  $J$  = 5.3 Hz, 1H), 5.05 (dd,  $J$  = 12.9, 5.4 Hz, 1H), 4.19 (d,  $J$  = 5.4 Hz, 2H), 3.61 (t,  $J$  = 5.4 Hz, 2H), 3.57-3.53 (m, 2H), 3.53-3.51 (m, 2H), 3.51-3.47 (m, 8H), 3.45 (d,  $J$  = 6.3 Hz, 2H), 3.42 (d,  $J$  = 5.7 Hz, 2H), 3.26 (dd,  $J$  = 11.4, 5.7 Hz, 2H), 2.88-2.80 (m, 1H), 2.60-2.51 (m, 2H), 2.06-1.97 (m, 1H).  $^{13}C$  NMR (101 MHz, DMSO- $d_6$ )  $\delta$  189.14, 172.78, 170.05, 168.86, 167.26, 158.61, 156.22, 155.22, 152.47, 146.36, 136.17, 135.80, 133.44, 132.04, 131.22, 130.75, 130.34, 124.68, 119.65, 119.10, 117.40, 116.58, 116.18, 110.62, 109.19, 100.60, 69.70, 68.91, 48.51, 43.54, 41.64, 30.95, 22.11. HRMS (ESI)  $m/z$ : calcd  $C_{44}H_{45}ClN_8O_{11}$   $[M+H]^+$ : 897.2969; found 897.2996.

**2-((5-(2-Chloro-4-phenoxybenzoyl)-7H-pyrrolo[2,3-d]pyrimidin-4-yl)amino)-N-(17-((2-(2,6-dioxopiperidin-3-yl)-1,3-dioxoisindolin-4-yl)amino)-3,6,9,12,15-pentaoxaheptadecyl)acetamide (4f).** Yield 13.2%.  $^1H$  NMR (400 MHz, DMSO- $d_6$ )  $\delta$  12.82 (s, 1H), 11.12 (s, 1H), 9.05 (s, 1H), 8.27 (s, 1H), 8.16 (t,  $J$  = 5.4 Hz, 1H), 7.67 (s, 1H), 7.62-7.54 (m, 2H), 7.50 (t,  $J$  = 7.9 Hz, 2H), 7.27 (t,  $J$  = 7.4 Hz, 1H), 7.25-7.17 (m, 3H), 7.15 (d,  $J$  = 8.6 Hz, 1H), 7.08-7.02 (m, 2H), 6.62 (s, 1H), 5.07 (dd,  $J$  = 12.9, 5.4 Hz, 1H), 4.21 (d,  $J$  = 5.4 Hz, 2H), 3.63 (t,  $J$  = 5.4 Hz, 2H), 3.58-3.51 (m, 10H), 3.48-3.43 (m, 10H), 3.28 (dd,  $J$  = 11.4, 5.7 Hz, 2H), 2.96-2.83 (m, 1H), 2.64-2.55 (m, 2H), 2.09-1.99 (m, 1H).  $^{13}C$  NMR (101 MHz, DMSO- $d_6$ )  $\delta$  189.16, 172.82, 170.08, 168.89, 167.26, 158.62, 155.20, 146.34, 136.19, 133.39, 132.04, 131.22, 130.76, 130.35, 124.70, 119.66, 119.11, 117.41, 116.60, 116.18, 110.63, 109.15, 100.59, 70.13, 68.90, 48.49, 43.53, 41.62, 30.94, 22.09. HRMS (ESI)  $m/z$ : calcd  $C_{46}H_{49}ClN_8O_{12}$   $[M+H]^+$ : 941.3231; found 941.3237.

**2-((5-(2-Chloro-4-phenoxybenzoyl)-7H-pyrrolo[2,3-d]pyrimidin-4-yl)amino)-N-(20-((2-(2,6-dioxopiperidin-3-yl)-1,3-dioxoisindolin-4-yl)amino)-3,6,9,12,15,18-hexaoxaicosyl)acetamide (4g).** Yield 23.0%.  $^1H$  NMR (400 MHz, DMSO- $d_6$ )  $\delta$  12.76 (s, 1H), 11.11 (s, 1H), 8.98 (t,  $J$  = 5.4 Hz, 1H), 8.25 (s, 1H), 8.14 (t,  $J$  = 5.6 Hz, 1H), 7.64 (s, 1H), 7.58 (t,  $J$  = 7.6 Hz, 2H), 7.52-7.44 (m, 2H), 7.30-7.23 (m, 1H), 7.22-7.16 (m, 3H), 7.14 (d,  $J$  = 8.6 Hz, 1H), 7.06-7.01 (m, 2H), 6.61 (t,  $J$  = 5.7 Hz, 1H), 5.06 (dd,  $J$  = 12.9, 5.4 Hz, 1H), 4.20 (d,  $J$  = 5.4 Hz, 2H), 3.62 (t,  $J$  = 5.4 Hz, 2H), 3.57-3.52 (m, 4H), 3.52-3.46 (m, 17H), 3.46-3.42 (m, 3H), 3.27 (dd,  $J$  = 11.4, 5.7 Hz, 2H), 2.95-2.83 (m, 1H), 2.62-2.50 (m, 2H), 2.08-1.98 (m, 1H).  $^{13}C$  NMR (101 MHz, DMSO- $d_6$ )  $\delta$  189.12, 172.78, 170.05, 168.89, 167.26, 158.59, 156.35, 155.22, 153.75, 152.57, 146.36, 136.18, 135.75, 133.47, 132.04, 131.22, 130.74, 130.34, 124.68, 119.65, 119.10, 117.41, 116.53, 116.18, 110.63, 109.18, 100.60, 69.99, 68.92, 48.51, 43.51, 41.64, 39.06-39.03, 38.73, 30.95, 22.11. HRMS (ESI)  $m/z$ : calcd  $C_{48}H_{53}ClN_8O_{13}$   $[M+H]^+$ : 985.3493; found 985.3518.

**2-((5-(2-Chloro-4-phenoxybenzoyl)-7H-pyrrolo[2,3-d]pyrimidin-4-yl)amino)-N-(23-((2-(2,6-dioxopiperidin-3-yl)-1,3-dioxoisindolin-4-yl)amino)-3,6,9,12,15,18,21-heptaotricosyl)acetamide (4h).** Yield 23.7%.  $^1H$  NMR (400 MHz, DMSO- $d_6$ )  $\delta$  12.74 (s, 1H), 11.10 (s, 1H), 8.96 (t,  $J$  = 5.4 Hz, 1H), 8.24 (s, 1H), 8.13 (t,  $J$  = 5.6 Hz, 1H), 7.63 (s, 1H), 7.57 (t,  $J$  = 8.1 Hz, 2H), 7.51-7.45 (m, 2H), 7.29-7.23 (m, 1H), 7.22-7.14 (m, 3H), 7.14 (d,  $J$  = 8.6 Hz, 1H), 7.08-7.01 (m, 2H), 6.60 (t,  $J$  = 5.7 Hz, 1H), 5.06 (dd,  $J$  = 12.9, 5.4 Hz, 1H), 4.19 (d,  $J$  = 5.4 Hz, 2H), 3.61 (t,  $J$  = 5.4 Hz, 2H), 3.58-3.48 (m, 4H), 3.53-3.45 (m, 21H), 3.46-3.42 (m, 3H), 3.27 (dd,  $J$  = 11.4, 5.7 Hz, 2H), 2.89-2.80 (m, 1H), 2.64-2.52 (m, 2H), 2.07-1.98 (m, 1H).  $^{13}C$  NMR (101 MHz, DMSO- $d_6$ )  $\delta$  189.10, 172.79, 170.05, 168.91, 167.26, 158.58, 156.41, 155.23, 153.84, 152.66, 146.36, 136.18, 135.77, 133.50, 132.04, 131.21,

130.73, 130.34, 124.67, 119.65, 119.10, 117.41, 116.50, 116.18, 110.63, 109.18, 100.61, 69.95, 68.92, 48.51, 43.49, 41.64, 38.61, 30.94, 22.10. HRMS (ESI)  $m/z$ : calcd  $C_{50}H_{57}ClN_8O_{14}$   $[M+H]^+$ : 1029.3756; found 1029.3763.

#### 4.5. General procedure for synthesis of compounds 5, 6

Step A: To a solution of (2-chloro-4-phenoxyphenyl)(4-chloro-7H-pyrrolo[2,3-d]pyrimidin-5-yl)methanone **B5** (0.50 g, 1.30 mmol) and *tert*-butyl ((1*S*,4*S*)-4-aminocyclohexyl)carbamate (0.31 g, 1.4 mmol) in IPA (30 mL) was added DIPEA (0.50 g, 0.39 mmol). The mixture was heated to reflux for 3 h. The solvent was evaporated in vacuo and the resulting solid was diluted with H<sub>2</sub>O (10 mL), the mixture solution was stirred at room temperature for 0.5 h and filtered. The crude product was purified by silica chromatography (200–300 mesh) using a solvent gradient of (10/1 to 1/3 petroleum ether/ethyl acetate) to give *tert*-butyl(4-((5-(2-chloro-4-phenoxybenzoyl)-7H-pyrrolo[2,3-d]pyrimidin-4-yl)amino)cyclohexyl)carbamate (0.60 g, 82.3%) as a white solid.

Step B: **4-(((1*S*,4*S*)-4-Aminocyclohexyl)amino)-7H-pyrrolo[2,3-d]pyrimidin-5-yl(2-chloro-4-phenoxyphenyl)methanone(5).** A solution of *tert*-butyl (4-((5-(2-chloro-4-phenoxybenzoyl)-7H-pyrrolo[2,3-d]pyrimidin-4-yl)amino)cyclohexyl)carbamate in 1:1 TFA/DCM was stirred at room temperature for 1 h. The solvents were evaporated under reduced pressure to give the intermediate **5** (TFA salt) that was used in the following reactions without further purification (95% yield).  $^1H$  NMR (400 MHz, DMSO- $d_6$ )  $\delta$  8.94 (d,  $J$  = 7.3 Hz, 1H), 8.22 (s, 1H), 7.62-7.56 (m, 2H), 7.51-7.45 (m, 2H), 7.26 (t,  $J$  = 7.4 Hz, 1H), 7.19 (dd,  $J$  = 9.3, 1.6 Hz, 3H), 7.03 (dd,  $J$  = 8.4, 2.4 Hz, 1H), 6.06 (s, 2H), 4.26 (s, 1H), 2.97 (s, 1H), 1.87 (d,  $J$  = 5.5 Hz, 2H), 1.78-1.70 (m, 4H), 1.63-1.52 (m, 2H).  $^{13}C$  NMR (101 MHz, DMSO- $d_6$ )  $\delta$  189.73, 158.59, 155.98, 155.25, 154.13, 152.67, 136.14, 133.45, 131.18, 130.83, 130.34, 124.67, 119.58, 119.12, 116.42, 116.20, 100.60, 48.56, 47.89, 44.77, 27.17, 26.04. HRMS (ESI)  $m/z$ : calcd  $C_{25}H_{24}ClN_5O_2$   $[M+H]^+$ : 462.1691; found 462.1701.

**1-(((1*S*,4*S*)-4-((5-(2-Chloro-4-phenoxybenzoyl)-7H-pyrrolo[2,3-d]pyrimidin-4-yl)amino)cyclohexyl)-3-ethylurea (6).** To a solution of **5** (0.11 g, 0.25 mmol) and DIPEA (5.0 equiv) in THF (5 mL) was added triphosgene (0.5 equiv). The mixture was stirred at 0 °C for 10 min. The reaction mixture was added ethanamine (1.2 equiv) dissolved in THF (5 mL). The resulting solution was stirred at 0 °C for 10 min at 0 °C, then was stirred at room temperature for another 0.5 h. The reaction mixture was diluted with water (10 mL) and extracted with ethyl acetate (3 × 15 mL). The combined organic layer was washed with brine solution, dried over Na<sub>2</sub>SO<sub>4</sub> and concentrated. The crude product was purified by silica chromatography (200–300 mesh) using a solvent gradient of (50/1 to 25/1 DCM/MeOH) to give compound **6** in 36.1% yield.  $^1H$  NMR (400 MHz, DMSO- $d_6$ )  $\delta$  12.74 (s, 1H), 8.93 (d,  $J$  = 7.5 Hz, 1H), 8.24 (s, 1H), 7.67-7.56 (m, 2H), 7.54-7.44 (m, 2H), 7.26 (dd,  $J$  = 10.6, 4.2 Hz, 1H), 7.19 (dd,  $J$  = 9.4, 1.7 Hz, 3H), 7.03 (dd,  $J$  = 8.4, 2.4 Hz, 1H), 5.95 (d,  $J$  = 7.7 Hz, 1H), 5.68 (t,  $J$  = 5.5 Hz, 1H), 4.24 (s, 1H), 3.60 (s, 1H), 3.06-2.94 (m, 2H), 1.79 (t,  $J$  = 8.8 Hz, 2H), 1.69 (d,  $J$  = 9.0 Hz, 4H), 1.61-1.49 (m, 2H), 0.97 (t,  $J$  = 7.2 Hz, 3H).  $^{13}C$  NMR (101 MHz, DMSO- $d_6$ )  $\delta$  189.79, 158.53, 157.26, 155.90, 155.28, 154.21, 152.67, 136.00, 133.53, 131.13, 130.76, 130.34, 124.65, 119.58, 119.11, 116.36, 100.55, 33.85, 28.85, 28.13, 15.67. HRMS (ESI)  $m/z$ : calcd  $C_{28}H_{29}ClN_6O_3$   $[M+H]^+$ : 533.2062; found 533.2085.

#### 4.6. General procedure for synthesis of compounds 6a-6e

**1-(((1*S*,4*S*)-4-((5-(2-Chloro-4-phenoxybenzoyl)-7H-pyrrolo[2,3-d]pyrimidin-4-yl)amino)cyclohexyl)-3-(4-((2-(2,6-dioxopiperidin-3-yl)-1,3-dioxoisindolin-4-yl)amino)butyl)urea (6a).** To a solution of 4-((4-aminobutyl)amino)-2-(2,6-

dioxopiperidin-3-yl)isoindoline-1,3-dione **A3b** (0.12 g, 0.36 mmol) and DIPEA (0.23 g, 1.8 mmol) in THF (5 mL) was added triphosgene (0.05 g, 0.18 mmol). The mixture was stirred at 0 °C for 10 min. The reaction mixture was added compound **5** (0.16 g, 0.36 mmol) dissolved in THF (5 mL). The resulting solution was stirred at 0 °C for 10 min, then was stirred at room temperature for another 0.5 h. The reaction mixture was diluted with water (10 mL) and extracted with ethyl acetate (3 × 15 mL). The combined organic layer was washed with brine solution, dried over Na<sub>2</sub>SO<sub>4</sub> and concentrated. The crude product was purified by silica chromatography (200–300 mesh) using a solvent gradient of (50/1 to 25/1 DCM/MeOH) to give compound **6a** in 21.7% yield. <sup>1</sup>H NMR (400 MHz, DMSO-*d*<sub>6</sub>) δ 12.73 (s, 1H), 11.10 (s, 1H), 8.92 (d, *J* = 7.5 Hz, 1H), 8.24 (s, 1H), 7.63 (s, 1H), 7.59 (d, *J* = 8.4 Hz, 1H), 7.57–7.54 (m, 1H), 7.51–7.46 (m, 2H), 7.29–7.23 (m, 1H), 7.21–7.17 (m, 3H), 7.10 (d, *J* = 8.6 Hz, 1H), 7.03 (dd, *J* = 8.5, 2.4 Hz, 1H), 6.99 (d, *J* = 7.0 Hz, 1H), 6.57 (t, *J* = 6.0 Hz, 1H), 5.95 (d, *J* = 7.7 Hz, 1H), 5.78 (t, *J* = 5.0 Hz, 1H), 5.05 (dd, *J* = 12.9, 5.4 Hz, 1H), 4.24 (s, 1H), 3.61 (s, 1H), 3.33–3.26 (m, 2H), 3.03 (dd, *J* = 12.5, 6.5 Hz, 2H), 2.92–2.85 (m, 1H), 2.63–2.52 (m, 2H), 2.08–1.97 (m, 1H), 1.79 (t, *J* = 8.6 Hz, 2H), 1.69 (d, *J* = 8.9 Hz, 4H), 1.61–1.50 (m, 4H), 1.44 (dd, *J* = 14.5, 6.9 Hz, 2H). <sup>13</sup>C NMR (101 MHz, DMSO-*d*<sub>6</sub>) δ 189.80, 172.79, 170.08, 168.88, 167.26, 158.54, 157.39, 155.90, 155.28, 154.21, 152.67, 146.35, 136.11, 133.52, 132.16, 131.13, 130.75, 130.33, 124.65, 119.58, 119.10, 117.18, 116.49, 116.23, 110.30, 100.55, 48.48, 41.53, 38.67, 30.94, 28.84, 28.13, 27.46, 26.17. HRMS (ESI) *m/z*: calcd C<sub>43</sub>H<sub>42</sub>ClN<sub>9</sub>O<sub>7</sub> [M+H]<sup>+</sup>: 832.2968; found 832.2946.

Following the procedures used to prepare compound **6a**, compounds **6b–6e** with different chain lengths were obtained by the same methods.

**1-((1*S*,4*S*)-4-((5-(2-Chloro-4-phenoxybenzoyl)-7*H*-pyrrolo [2,3-*d*]pyrimidin-4-yl)amino)cyclohexyl)-3-(2-(2-(2-(2-(2-(2,6-dioxopiperidin-3-yl)-1,3-dioxoisindolin-4-yl)amino)ethoxy)ethoxy)ethyl)urea (6b)**. Yield 23.1%. <sup>1</sup>H NMR (400 MHz, DMSO-*d*<sub>6</sub>) δ 12.73 (s, 1H), 11.11 (s, 1H), 8.91 (d, *J* = 7.5 Hz, 1H), 8.24 (s, 1H), 7.62 (s, 1H), 7.59 (d, *J* = 8.4 Hz, 1H), 7.57–7.53 (m, 1H), 7.51–7.45 (m, 2H), 7.29–7.23 (m, 1H), 7.21–7.16 (m, 3H), 7.13 (d, *J* = 8.6 Hz, 1H), 7.05–7.00 (m, 2H), 6.61 (t, *J* = 6.0 Hz, 1H), 6.14 (d, *J* = 7.7 Hz, 1H), 5.81 (t, *J* = 5.0 Hz, 1H), 5.06 (dd, *J* = 12.9, 5.4 Hz, 1H), 4.23 (s, 1H), 3.62 (t, *J* = 5.4 Hz, 3H), 3.57 (dd, *J* = 5.8, 3.1 Hz, 2H), 3.53 (dd, *J* = 5.6, 3.0 Hz, 2H), 3.46 (dd, *J* = 11.0, 5.5 Hz, 2H), 3.39 (t, *J* = 5.6 Hz, 2H), 3.19–3.11 (m, 2H), 2.92–2.84 (m, 1H), 2.65–2.52 (m, 2H), 2.10–1.94 (m, 1H), 1.80 (t, *J* = 8.5 Hz, 2H), 1.69 (d, *J* = 9.0 Hz, 4H), 1.60–1.52 (m, 2H). <sup>13</sup>C NMR (101 MHz, DMSO-*d*<sub>6</sub>) δ 189.78, 172.77, 170.06, 168.89, 167.25, 158.53, 157.28, 155.90, 155.27, 154.21, 152.67, 146.34, 136.07, 133.52, 132.05, 131.13, 130.75, 130.32, 124.64, 119.57, 119.09, 117.37, 116.49, 116.22, 110.62, 109.21, 100.55, 70.19, 69.61, 68.84, 48.51, 41.63, 30.94, 28.86, 28.08, 22.10. HRMS (ESI) *m/z*: calcd C<sub>45</sub>H<sub>46</sub>ClN<sub>9</sub>O<sub>9</sub> [M+H]<sup>+</sup>: 892.3180; found 892.3190.

**1-((1*S*,4*S*)-4-((5-(2-Chloro-4-phenoxybenzoyl)-7*H*-pyrrolo [2,3-*d*]pyrimidin-4-yl)amino)cyclohexyl)-3-(2-(2-(2-(2-(2-(2,6-dioxopiperidin-3-yl)-1,3-dioxoisindolin-4-yl)amino)ethoxy)ethoxy)ethoxy)ethyl)urea (6c)**. Yield 17.9%. <sup>1</sup>H NMR (400 MHz, DMSO-*d*<sub>6</sub>) δ 12.73 (s, 1H), 11.11 (s, 1H), 8.92 (d, *J* = 7.4 Hz, 1H), 8.24 (s, 1H), 7.62 (s, 1H), 7.59 (d, *J* = 8.4 Hz, 1H), 7.57–7.54 (m, 1H), 7.51–7.45 (m, 2H), 7.28–7.23 (m, 1H), 7.21–7.16 (m, 3H), 7.12 (d, *J* = 8.6 Hz, 1H), 7.06–7.00 (m, 2H), 6.60 (t, *J* = 5.7 Hz, 1H), 6.14 (d, *J* = 7.6 Hz, 1H), 5.81 (t, *J* = 5.6 Hz, 1H), 5.06 (dd, *J* = 12.9, 5.4 Hz, 1H), 4.23 (s, 1H), 4.15–4.08 (m, 1H), 3.61 (t, *J* = 5.4 Hz, 3H), 3.56 (dd, *J* = 6.2, 3.5 Hz, 2H), 3.54–3.50 (m, 4H), 3.49 (dd, *J* = 5.3, 2.7 Hz, 3H), 3.47–3.43 (m, 2H), 3.20–3.10 (m, 2H), 2.94–2.83 (m, 1H), 2.63–2.53 (m, 2H), 2.07–1.96 (m, 1H), 1.80 (t, *J* = 8.4 Hz, 2H), 1.69 (d, *J* = 8.8 Hz, 4H), 1.61–1.51 (m, 2H). <sup>13</sup>C NMR (101 MHz, DMSO-*d*<sub>6</sub>) δ 189.78, 172.78, 170.05, 168.89, 167.25, 158.53, 157.28, 155.90, 155.27, 154.21, 152.66, 146.34, 136.06, 135.93–135.74, 133.52, 132.04, 131.14, 130.75, 130.32, 124.63, 119.56, 119.09, 117.37, 116.49, 116.22, 110.62, 109.19, 100.55, 70.13, 69.77,

69.54, 68.83, 48.54, 41.63, 30.94, 28.85, 28.07, 22.11. HRMS (ESI) *m/z*: calcd C<sub>47</sub>H<sub>50</sub>ClN<sub>9</sub>O<sub>10</sub> [M+H]<sup>+</sup>: 936.3442; found 936.3463.

**1-((1*S*,4*S*)-4-((5-(2-Chloro-4-phenoxybenzoyl)-7*H*-pyrrolo [2,3-*d*]pyrimidin-4-yl)amino)cyclohexyl)-3-(14-((2-(2,6-dioxopiperidin-3-yl)-1,3-dioxoisindolin-4-yl)amino)-3,6,9,12-tetraoxatetradecyl)urea (6d)**. Yield 30.1%. <sup>1</sup>H NMR (400 MHz, DMSO-*d*<sub>6</sub>) δ 12.74 (s, 1H), 11.11 (s, 1H), 8.91 (d, *J* = 7.5 Hz, 1H), 8.23 (s, 1H), 7.61 (s, 1H), 7.60–7.54 (m, 2H), 7.51–7.45 (m, 2H), 7.29–7.23 (m, 1H), 7.18 (dd, *J* = 7.3, 1.6 Hz, 3H), 7.13 (d, *J* = 8.6 Hz, 1H), 7.07–7.00 (m, 2H), 6.60 (t, *J* = 5.7 Hz, 1H), 6.14 (d, *J* = 7.7 Hz, 1H), 5.80 (dd, *J* = 12.9, 5.4 Hz, 1H), 5.06 (dd, *J* = 12.9, 5.4 Hz, 1H), 4.23 (s, 1H), 3.60 (t, *J* = 5.4 Hz, 3H), 3.57–3.42 (m, 16H), 3.19–3.10 (m, 2H), 2.93–2.80 (m, 1H), 2.63–2.52 (m, 2H), 2.07–1.96 (m, 1H), 1.80 (t, *J* = 8.4 Hz, 2H), 1.69 (d, *J* = 9.0 Hz, 4H), 1.60–1.50 (m, 2H). <sup>13</sup>C NMR (101 MHz, DMSO-*d*<sub>6</sub>) δ 189.77, 172.79, 170.05, 168.89, 167.26, 158.53, 157.28, 155.26, 154.20, 152.67, 146.35, 136.09, 133.52, 132.03, 131.13, 130.75, 130.33, 124.65, 119.57, 119.08, 117.39, 116.48, 116.22, 110.63, 109.18, 100.55, 70.12, 69.76, 69.52, 68.82, 48.50, 41.63, 30.94, 28.84, 28.07, 22.10. HRMS (ESI) *m/z*: calcd C<sub>49</sub>H<sub>54</sub>ClN<sub>9</sub>O<sub>11</sub> [M+H]<sup>+</sup>: 980.3704; found 980.3712.

**1-((1*S*,4*S*)-4-((5-(2-Chloro-4-phenoxybenzoyl)-7*H*-pyrrolo [2,3-*d*]pyrimidin-4-yl)amino)cyclohexyl)-3-(17-((2-(2,6-dioxopiperidin-3-yl)-1,3-dioxoisindolin-4-yl)amino)-3,6,9,12,15-pentaoxaheptadecyl)urea (6e)**. Yield 19.5%. <sup>1</sup>H NMR (400 MHz, DMSO-*d*<sub>6</sub>) δ 12.73 (s, 1H), 11.11 (s, 1H), 8.91 (d, *J* = 7.4 Hz, 1H), 8.23 (s, 1H), 7.62 (s, 1H), 7.61–7.54 (m, 2H), 7.52–7.44 (m, 2H), 7.30–7.22 (m, 1H), 7.20–7.18 (m, 2H), 7.17 (s, 1H), 7.13 (d, *J* = 8.6 Hz, 1H), 7.07–7.00 (m, 2H), 6.60 (t, *J* = 5.7 Hz, 1H), 6.14 (d, *J* = 7.7 Hz, 1H), 5.81 (t, *J* = 5.6 Hz, 1H), 5.06 (dd, *J* = 12.9, 5.4 Hz, 1H), 4.23 (s, 1H), 3.61 (t, *J* = 5.4 Hz, 3H), 3.60–3.50 (m, 2H), 3.53–3.50 (m, 2H), 3.50 (s, 4H), 3.48 (s, 6H), 3.46 (dd, *J* = 9.3, 3.7 Hz, 2H), 3.37 (t, *J* = 5.6 Hz, 2H), 3.34 (s, 2H), 3.14 (q, *J* = 5.5 Hz, 2H), 2.93–2.84 (m, 1H), 2.63–2.52 (m, 2H), 2.09–1.97 (m, 1H), 1.80 (t, *J* = 8.5 Hz, 2H), 1.69 (d, *J* = 8.9 Hz, 4H), 1.62–1.51 (m, 2H). <sup>13</sup>C NMR (101 MHz, DMSO-*d*<sub>6</sub>) δ 189.76, 172.79, 170.05, 168.89, 158.52, 157.25, 155.89, 155.27, 154.20, 152.68, 146.35, 136.18, 133.53, 132.04, 131.13, 130.76, 130.33, 124.64, 119.56, 119.09, 117.39, 116.48, 116.22, 110.62, 109.17, 100.55, 70.14, 69.75, 69.52, 68.82, 48.50, 41.63, 30.94, 28.86, 28.06, 22.10. HRMS (ESI) *m/z*: calcd C<sub>51</sub>H<sub>58</sub>ClN<sub>9</sub>O<sub>12</sub> [M+H]<sup>+</sup>: 1024.3966; found 1024.3967.

#### 4.7. Cell lines and cell culture

JeKo-1, BTK<sup>WT</sup> TMD8 cells and BTK<sup>C481S</sup> TMD8 cells were kindly provided by Shanghai Meizer Pharmaceuticals Co., Ltd. Cells were cultured in RPMI-1640 medium supplemented with 20% fetal bovine serum and 1% penicillin and streptomycin. Cells were cultured at 37 °C with 5% CO<sub>2</sub>.

#### 4.8. Cell proliferation assay

Effects of compounds on cell viability were determined by using cell counting kit-8 (CCK-8, Meilun MA0218). BTK<sup>WT</sup> TMD8 cells and BTK<sup>C481S</sup> TMD8 cells were seeded in 96-well plates at a density of 10<sup>4</sup> cells per well in triplicate. Next day, chemicals were treated in each well to a final concentration of 1.0 nM, 3.0 nM, 10.0 nM, 30.0 nM, 100.0 nM, 300.0 nM, 1000.0 nM. The viability was quantified compared to DMSO alone. After the treatment of compound for 72 h, 10 μL CCK-8 was added and incubated for 4 h. The absorbance was read at 450 nm using a micro plate reader (TECAN Infinite M200pro Switzerland).

#### 4.9. Western blot assay

Equivalent amounts of protein for each sample were separated by 8% SDS-PAGE gels and transferred to the polyvinylidene

difluoride membranes. Then, membrane was blocked in 5% BSA (Albumin from bovine serum) in the TBST for 1 h, incubated with a primary antibody overnight at 4 °C and treated with secondary antibody for 1 h at room temperature. The band signals were imaged with extreme hypersensitivity ECL chemiluminescence kit. The total gray of each band was quantified via the ImageJ software. DC<sub>50</sub> (the concentration leading to 50% target protein degradation) and D<sub>max</sub> (the maximum protein degradation level) were used to quantify the target protein degradation ability of PROTACs. The final concentrations of compounds used in DC<sub>50</sub> determination were 1.6 nM, 8.0 nM, 40.0 nM, 200.0 nM and 1000.0 nM, respectively.

#### 4.10. BTK inhibition

The compound was serially diluted for a series of concentrations (0.04 nM, 0.15 nM, 1.0 nM, 2.0 nM, 10.0 nM, 39.0 nM, 156.0 nM, 625.0 nM, 2500.0 nM, 10000 nM) as designed. Then, 90 µL of 1 × kinase buffer (50 mM HEPES, pH 7.5, 0.0015% Brij-35) was added into each well of the intermediate plate. Transfer 5 µL of each well from the 96-well intermediate plate to a 384-well plate in duplicates. At last, prepare BTK enzyme solution (Carna, Cat.No 08–180, Lot. No 14CBS-0619D), peptide FAM-P2 solution (GL Biochem, Cat. No. 112394, Lot. No. P131014-XP112394); ATP (Sigma, Cat. No. A7699-1G, CAS No. 987-65-5) and 5 µL of compound in 10% DMSO (Sigma, Cat. No. D2650, Lot. No. 474382) for the Kinase reaction. The reaction system was incubated at room temperature for 10 min and then stopped by adding 25 µL of stop buffer (100 mM HEPES, pH 7.5; 0.015% Brij-35; 0.2% Coating Reagent #3; 50 mM EDTA (Sigma, Cat. No. E5134, CAS No. 60-00-4)). Detect them with a micro plate reader and fit the data in XL fit excel to obtain IC<sub>50</sub> values.

#### 4.11. Statistical analysis

Statistical tests and the associated error bars are identified in the corresponding figure legends. Typical replicate numbers describe the number of technical replicates analyzed in a single experiment.

#### Declaration of competing interest

The authors declare that they have no known competing financial interests or personal relationships that could have appeared to influence the work reported in this paper.

#### Acknowledgements

This work was supported by Natural National Science Foundation of China (Grant Numbers: 81874287; 81973163; 82003577), Shanghai Bio-pharmaceutical Science and Technology Supporting Plan (Grant Number: 19431900100), National Science and Technology Major Project (Grant Number: 2018ZX09711002-003-014) and Natural Science Foundation of Shanghai (Grant Number: 19ZR1436700).

#### Appendix A. Supplementary data

Supplementary data to this article can be found online at <https://doi.org/10.1016/j.ejmech.2021.113820>.

#### Author contributions statement

Y.Z. and Y.S. contributed equally to this work. N.S., Y.Z., Y.S., Q.X. and Y.W. drafted the manuscript, conceived the experiments, oversaw the experimental design, and provided study supervision. Y.Z., Y.B. and L.L. carried out the synthesis and characterization of

the compounds. Y.S., J.L., and Z.C. performed the biological activity studies. All authors reviewed the manuscript.

#### References

- [1] S.H. Swerdlow, E. Campo, S.A. Pileri, N.L. Harris, H. Stein, R. Siebert, R. Advani, M. Ghielmini, G.A. Salles, A.D. Zelenetz, E.S. Jaffe, The 2016 revision of the World Health Organization classification of lymphoid neoplasms, *Blood* 127 (2016) 2375–2390.
- [2] M. Deweers, M.C.M. Verschuren, M.E.M. Kraakman, R.G.J. Mensink, R.K.B. Schuurman, J.J.M. Vandongen, R.W. Hendriks, The bruton tyrosine kinase gene is expressed throughout B-cell differentiation, from early precursor B-cell stages preceding immunoglobulin gene rearrangement up to mature B-cell stages, *Eur. J. Immunol.* 23 (1993) 3109–3114.
- [3] S.P. Singh, F. Dammeijer, R.W. Hendriks, Role of bruton's tyrosine kinase in B cells and malignancies, *Mol. Cancer* 17 (2018) 57–80.
- [4] R.W. Hendriks, S. Yuvaraj, L.P. Kil, Targeting bruton's tyrosine kinase in B cell malignancies, *Nat. Rev. Cancer* 14 (2014) 219–232.
- [5] L.A. Honigberg, A.M. Smith, M. Sirisawad, E. Verner, D. Loury, B. Chang, S. Li, Z. Pan, D.H. Thamm, R.A. Miller, J.J. Buggy, The bruton tyrosine kinase inhibitor PCI-32765 blocks B-cell activation and is efficacious in models of autoimmune disease and B-cell malignancy, *P. Natl. Acad. Sci. U.S.A.* 107 (2010) 13075–13080.
- [6] C. da Cunha-Bang, C.U. Niemann, Targeting bruton's tyrosine kinase across B-cell malignancies, *Drugs* 78 (2018) 1653–1663.
- [7] Y. Guo, Y. Liu, N. Hu, D. Yu, C. Zhou, G. Shi, B. Zhang, M. Wei, J. Liu, L. Luo, Z. Tang, H. Song, Y. Guo, X. Liu, D. Su, S. Zhang, X. Song, X. Zhou, Y. Hong, S. Chen, Z. Cheng, S. Young, Q. Wei, H. Wang, Q. Wang, L. Lv, F. Wang, H. Xu, H. Sun, H. Xing, N. Li, W. Zhang, Z. Wang, G. Liu, Z. Sun, D. Zhou, W. Li, L. Wang, Z. Wang, Discovery of zanubrutinib (BGB-3111), a novel, potent, and selective covalent inhibitor of bruton's tyrosine kinase, *J. Med. Chem.* 62 (2019) 7923–7940.
- [8] W.H. Wilson, R.M. Young, R. Schmitz, Y. Yang, S. Pittaluga, G. Wright, C.-J. Lih, P.M. Williams, A.L. Shaffer, J. Gerecitano, S. de Vos, A. Goy, V.P. Kenkre, P.M. Barr, K.A. Blum, A. Shustov, R. Advani, N.H. Fowler, J.M. Vose, R.L. Elstrom, T.M. Habermann, J.C. Barrientos, J. McGreiv, M. Fardis, B.Y. Chang, F. Clow, B. Munneke, D. Moussa, D.M. Beaupre, L.M. Staudt, Targeting B cell receptor signaling with ibrutinib in diffuse large B cell lymphoma, *Nat. Med.* 21 (2015) 922–926.
- [9] J.A. Woyach, R.R. Furman, T.-M. Liu, H.G. Ozer, M. Zapatka, A.S. Ruppert, L. Xue, D.H.-H. Li, S.M. Steggerda, M. Versele, S.S. Dave, J. Zhang, A.S. Yilmaz, S.M. Jaglowski, K.A. Blum, A. Lozanski, G. Lozanski, D.F. James, J.C. Barrientos, P. Lichter, S. Stilgenbauer, J.J. Buggy, B.Y. Chang, A.J. Johnson, J.C. Byrd, Resistance mechanisms for the bruton's tyrosine kinase inhibitor ibrutinib, *N. Engl. J. Med.* 370 (2014) 2286–2294.
- [10] H.Y. Estupinan, Q. Wang, A. Berglof, G.C.P. Schaafsma, Y. Shi, L. Zhou, D.K. Mohammad, L. Yu, M. Vihinen, R. Zain, C.I.E. Smith, BTK gatekeeper residue variation combined with cysteine 481 substitution causes super-resistance to irreversible inhibitors acalabrutinib, ibrutinib and zanubrutinib, *Leukemia* 35 (2021) 1317–1329.
- [11] A.D. Buhimschi, H.A. Armstrong, M. Toure, S. Jaime-Figueroa, T.L. Chen, A.M. Lehman, J.A. Woyach, A.J. Johnson, J.C. Byrd, C.M. Crews, Targeting the C481S ibrutinib-resistance mutation in bruton's tyrosine kinase using PROTAC-mediated degradation, *Biochemistry* 57 (2018) 3564–3575.
- [12] C.V. Dang, E.P. Reddy, K.M. Shokat, L. Soucek, Drugging the 'undruggable' cancer targets, *Nat. Rev. Cancer* 17 (2017) 502–508.
- [13] P.P. Chamberlain, L.G. Hamann, Development of targeted protein degradation therapeutics, *Nat. Chem. Biol.* 15 (2019) 937–944.
- [14] A.C. Lai, C.M. Crews, Induced protein degradation: an emerging drug discovery paradigm, *Nat. Rev. Drug Discov.* 16 (2017) 101–114.
- [15] C.J. Gerry, S.L. Schreiber, Unifying principles of bifunctional, proximity-inducing small molecules, *Nat. Chem. Biol.* 16 (2020) 369–378.
- [16] Y. Sun, N. Ding, Y. Song, Z. Yang, W. Liu, J. Zhu, Y. Rao, Degradation of bruton's tyrosine kinase mutants by PROTACs for potential treatment of ibrutinib-resistant non-Hodgkin lymphomas, *Leukemia* 33 (2019) 2105–2110.
- [17] W.-H. Guo, X. Qi, X. Yu, Y. Liu, C.-I. Chung, F. Bai, X. Lin, D. Lu, L. Wang, J. Chen, L.H. Su, K.J. Nomie, F. Li, M.C. Wang, X. Shu, J.N. Onuchic, J.A. Woyach, M.L. Wang, J. Wang, Enhancing intracellular accumulation and target engagement of PROTACs with reversible covalent chemistry, *Nat. Commun.* 11 (2020) 4268–4284.
- [18] R. Gabizon, A. Shrager, P. Gehrtz, E. Livnah, Y. Shorer, N. Gurwicz, L. Avram, T. Unger, H. Aharoni, S. Albeck, A. Brandis, Z. Shulman, B.-Z. Katz, Y. Herishanu, N. London, Efficient targeted degradation via reversible and irreversible covalent PROTACs, *J. Am. Chem. Soc.* 142 (2020) 11734–11742.
- [19] A. Zorba, N. Chuong, Y. Xu, J. Starr, K. Borzilleri, J. Smith, H. Zhu, K.A. Farley, W. Ding, J. Schiemer, X. Feng, J.S. Chang, D.P. Uccello, J.A. Young, C.N. Garcia-Irrizar, L. Czabaniuk, B. Schuff, R. Oliver, J. Montgomery, M.M. Hayward, J. Coe, J. Chen, M. Niosi, S. Luthra, J.C. Shah, A. El-Kattan, X. Qiu, G.M. West, M.C. Noe, V. Shanmugasundaram, A.M. Gilbert, M.F. Brown, M.F. Calabrese, Delineating the role of cooperativity in the design of potent PROTACs for BTK, *Proc. Natl. Acad. Sci. U.S.A.* 115 (2018) E7285–E7292.
- [20] G. Xue, J. Chen, L. Liu, D. Zhou, Y. Zuo, T. Fu, Z. Pan, Protein degradation through covalent inhibitor-based PROTACs, *Chem. Commun.* 56 (2020)

- 1521–1524.
- [21] S. Jaime-Figueroa, A.D. Buhimschi, M. Toure, J. Hines, C.M. Crews, Design, synthesis and biological evaluation of Proteolysis Targeting Chimeras (PROTACs) as a BTK degraders with improved pharmacokinetic properties, *Bioorg. Med. Chem. Lett.* 30 (2020) 126877–126909.
- [22] C.P. Tinworth, H. Lithgow, L. Dittus, Z.I. Bassi, S.E. Hughes, M. Muelbaier, H. Dai, I.E.D. Smith, W.J. Kerr, G.A. Burley, M. Bantscheff, J.D. Harling, PROTAC-mediated degradation of bruton's tyrosine kinase is inhibited by covalent binding, *ACS Chem. Biol.* 14 (2019) 342–347.
- [23] D. Gu, H. Tang, J. Wu, J. Li, Y. Miao, Targeting bruton tyrosine kinase using non-covalent inhibitors in B cell malignancies, *J. Hematol. Oncol.* 14 (2021) 40–55.
- [24] S.D. Reiff, R. Mantel, L.L. Smith, S. McWhorter, V.M. Goettl, A.J. Johnson, S. Eathiraj, G. Abbadessa, B. Schwartz, J.C. Byrd, J.A. Woyach, The bruton's tyrosine kinase (BTK) inhibitor ARQ 531 effectively inhibits wild type and C481S mutant BTK and is superior to ibrutinib in a mouse model of chronic lymphocytic leukemia, *Blood* 128 (2016), 3232–3232.
- [25] S.D. Reiff, R. Mantel, L.L. Smith, J.T. Greene, E.M. Muhowski, C.A. Fabian, V.M. Goettl, M. Tran, B.K. Harrington, K.A. Rogers, F.T. Awan, K. Maddocks, L. Andritsos, A.M. Lehman, D. Sampath, R. Lapalombella, S. Eathiraj, G. Abbadessa, B. Schwartz, A.J. Johnson, J.C. Byrd, J.A. Woyach, The BTK inhibitor ARQ 531 targets ibrutinib-resistant CLL and richter transformation, *Cancer Discov.* 8 (2018) 1300–1315.
- [26] X. Sun, H. Gao, Y. Yang, M. He, Y. Wu, Y. Song, Y. Tong, Y. Rao, PROTACs: great opportunities for academia and industry, *Signal Transduct. Targeted Ther.* 4 (2019) 64–97.
- [27] C. Steinebach, H. Kehm, S. Lindner, V. Lan Phuong, S. Koepff, A.L. Marmol, C. Weiler, K.G. Wagner, M. Reichenzeller, J. Kroenke, M. Guetschow, PROTAC-mediated crosstalk between E3 ligases, *Chem. Commun.* 55 (2019) 1821–1824.
- [28] C. Steinebach, I. Sosic, S. Lindner, A. Bricelj, F. Kohl, Y.L.D. Ng, M. Monschke, K.G. Wagner, J. Kroenke, M. Guetschow, A MedChem toolbox for cereblon-directed PROTACs, *MedChemComm* 10 (2019) 1037–1041.
- [29] B. George, S.M. Chowdhury, A. Hart, A. Sircar, S.K. Singh, U.K. Nath, M. Mamgain, N.K. Singhal, L. Sehgal, N. Jain, Ibrutinib resistance mechanisms and treatment strategies for B-cell lymphomas, *Cancers* 12 (2020) 1328–1359.
- [30] V.G. Klein, C.E. Townsend, A. Testa, M. Zengerle, C. Maniaci, S.J. Hughes, K.-H. Chan, A. Ciulli, R.S. Lokey, Understanding and improving the membrane permeability of VH032-based PROTACs, *ACS Med. Chem. Lett.* 11 (2020) 1732–1738.
- [31] S.D. Edmondson, B. Yang, C. Fallan, Proteolysis targeting chimeras (PROTACs) in 'beyond rule-of-five' chemical space: recent progress and future challenges, *Bioorg. Med. Chem. Lett.* 29 (2019) 1555–1564.
- [32] H.J. Maple, N. Clayden, A. Baron, C. Stacey, R. Felix, Developing degraders: principles and perspectives on design and chemical space, *MedChemComm* 10 (2019) 1755–1764.